RSC Advances

REVIEW

View Article Online
View Journal | View Issue

Cite this: *RSC Adv.*, 2026, **16**, 34

MXenes in diabetes: diagnostic and therapeutic applications

Meisam Samadzadeh,†[a] Mahshid Danesh,†[b] Atefeh Zarepour,[c] Arezoo Khosravi,[de] Ali Zarrabi *[f] and Siavash Iravani *[g]

This review highlights the promising role of MXenes and their composites in diabetes management, emphasizing their dual utility in diagnostics and therapeutics. MXenes' exceptional electrical conductivity, hydrophilicity, mechanical robustness, and tunable surface chemistry facilitate the design of sensitive and selective biosensors for real-time and non-invasive monitoring of key diabetes biomarkers like glucose and acetone. Therapeutically, MXene-based materials enhance healing of diabetic complications such as foot ulcers by modulating inflammation, scavenging reactive oxygen species, promoting angiogenesis, and supporting tissue regeneration *via* multifunctional hydrogels, patches, and scaffolds. Despite these advances, challenges remain including environmentally harmful synthesis methods, limited scalability, oxidation-induced instability under physiological conditions, and insufficient biocompatibility data. Future efforts are directed toward developing greener and scalable synthesis routes, improving MXene stability through surface modifications, and integrating MXenes with cutting-edge technologies such as wearable devices, 3D bioprinting, and bioelectronics. Additionally, the review uniquely explores the incorporation of artificial intelligence and machine learning techniques to enable personalized and adaptive diabetes management. By providing a comprehensive synthesis of recent developments, current limitations, and innovative future directions, this review offers novel insights aimed at accelerating the clinical translation of MXene-based platforms to significantly enhance diabetes diagnosis and treatment.

Received 22nd August 2025
Accepted 12th December 2025

DOI: 10.1039/d5ra06236e

rsc.li/rsc-advances

1 Introduction

Diabetes mellitus is a long-term metabolic condition marked by consistently high blood sugar levels, which occurs due to impaired insulin production, insulin resistance, or a combination of both.[1] Recognized as one of the most widespread non-communicable illnesses, diabetes currently impacts more than 400 million people globally, with numbers steadily increasing.[2] This rise is largely attributed to factors such as physical inactivity, unhealthy eating patterns, and inherited genetic risks.[3] The World Health Organization (WHO) identifies diabetes as a critical public health concern, citing its potential to cause severe complications like heart disease, kidney dysfunction, nerve damage, and vision impairment. Effective management of diabetes requires timely and accurate diagnosis, as well as continuous glucose monitoring to maintain glycemic control and prevent severe complications.[4]

Traditional methods for diabetes diagnosis and glucose monitoring involve biochemical assays such as fasting blood glucose (FBG), oral glucose tolerance tests (OGTT), and glycated hemoglobin (HbA1c) measurements.[5] Although these methods provide valuable clinical insights, they suffer from several limitations, including invasiveness, patient discomfort, and delayed results. On the other hand, the conventional self-monitoring blood glucose (SMBG) technique relies on finger-prick tests, which are not only painful but also provide discrete rather than continuous glucose data, making it challenging to detect sudden glycemic fluctuations.[6] Recently, nanomaterials have gained attention in diabetes research, offering innovative approaches for both diagnosis and treatment. Their use in biomedicine has demonstrated notable benefits across various diabetes-related applications, including biomarker detection, glucose regulation, insulin-like activity, and complication prevention.[7] So far, different types of nanomaterials have been used for detection and treatment of diabetes due to their interesting features.[8,9] For example, graphene

[a]*Department of Molecular Biology and Genetics, Faculty of Engineering and Natural Sciences, Istinye University, Istanbul 34396, Türkiye*
[b]*Department of Bioinformatics, Biocenter, University of Würzburg, Am Hubland, 97074 Würzburg, Germany*
[c]*Department of Biology, Faculty of Arts and Sciences, Kocaeli University, 41001, İzmit, Kocaeli, Türkiye*
[d]*Department of Genetics and Bioengineering, Faculty of Engineering and Natural Sciences, Istanbul Okan University, Istanbul 34959, Türkiye*
[e]*Graduate School of Biotechnology and Bioengineering, Yuan Ze University, Taoyuan 320315, Taiwan*
[f]*Department of Biomedical Engineering, Faculty of Engineering and Natural Sciences, Istinye University, Istanbul 34396, Türkiye. E-mail: alizarrabi@gmail.com*
[g]*Independent Researcher, W Nazar ST, Boostan Ave, Isfahan, Iran. E-mail: siavashira@gmail.com*
† Authors with the same contribution.

and its derivatives provide high surface area and excellent electrochemical properties for glucose sensing; gold and silver nanoparticles are widely employed for biosensing and drug delivery due to their stability and facile functionalization; quantum dots enable sensitive fluorescence-based detection, while polymeric nanoparticles facilitate controlled insulin delivery.[10–16] In this context, MXene-based materials get significant attention in recent research. These are a new group of two-dimensional (2D) transition metal carbides, nitrides, and carbonitrides originate from MAX phases, a family of layered ternary compounds composed of a transition metal (M), an element from group A, and either carbon or nitrogen (X).[17] Through the selective removal of the A-layer, typically achieved using hydrofluoric acid (HF) or alternative etching techniques, MXenes are produced with surface terminations such as hydroxyl (OH), fluorine (F), or oxygen (O).[18] These functional groups play a crucial role in determining the chemical properties and application potential of MXenes. Their unique properties make them promising candidates for energy storage, catalysis, and biomedical applications. Recent advancements in synthesis methods aim to improve efficiency and safety, replacing traditional HF etching with alternative approaches like ammonium bifluoride (NH_4HF_2) or lithium fluoride with hydrochloric acid (LiF + HCl). These refined techniques enhance MXene quality, offering improved scalability for future applications in biosensors, supercapacitors, and catalysis.[19] Among various 2D nanomaterials, MXenes are particularly promising because they combine high electrical conductivity, a large accessible surface area, intrinsic hydrophilicity, and tunable surface chemistry, features that facilitate biomolecule immobilization, efficient electrochemical response, and high drug- or biomarker-loading capacity.[20,21] For instance, MXene-based platforms have demonstrated superior performance in electrochemical biosensing and drug delivery compared to traditional carbon-based or semiconducting 2D materials, which often require extensive surface modification to achieve comparable hydrophilicity and biocompatibility. Recent reviews have summarized how these properties make MXenes especially promising for biomedical applications such as sensing, imaging, and therapy.[22–24]

In diagnostics, MXene-based biosensors enable highly sensitive, selective, and rapid detection of glucose and other diabetes-related biomarkers, often through non-enzymatic electrochemical sensing platforms.[25,26] These sensors exhibit wide linearity, low detection limits, and high repeatability, making them suitable for real-time monitoring and mass screening of diabetic patients. Additionally, MXenes enhance wearable sensor technologies, facilitating continuous and non-invasive diabetes monitoring. Their tunable surface chemistry allows for customization to improve sensor performance and biocompatibility, positioning MXenes as a next-generation material in diabetes diagnostics.[27]

Therapeutically, MXenes and their composites show significant potential in addressing diabetic complications, particularly diabetic foot ulcers, which are a major cause of morbidity in diabetes.[28] MXene-based materials, such as hydrogels and microneedle patches, promote healing of diabetic wounds by reducing local glucose levels, providing oxygen delivery, and generating mild hyperthermia to stimulate tissue regeneration.[29] They also exhibit anti-inflammatory and antioxidant properties by scavenging reactive oxygen species and modulating immune responses, which are crucial for chronic wound repair.[30,31] Furthermore, MXene composites support tissue regeneration in diabetic related disease by enhancing angiogenesis and macrophage polarization, thereby accelerating healing processes.[32,33] Despite these promising advances, challenges remain in scaling up MXene synthesis, ensuring long-term biocompatibility, and fully understanding the *in vivo* behavior, which are critical for clinical translation of MXene-based diabetes therapies.[34]

This review explores an overview of MXene-based composites and their multifaceted role in diabetes management, encompassing both diagnostic and therapeutic applications. The diagnostic section delves into MXene-based glucose sensing technologies, their integration into wearable continuous monitoring devices, and their superiority over traditional finger-prick methods. Additionally, the potential of MXenes in early biomarker detection is discussed, emphasizing their ability to enhance early-stage diabetes diagnosis. The therapeutic section highlights MXenes as innovative drug delivery systems, their potential in insulin delivery enhancement, and their contributions to tissue engineering and wound healing in diabetic patients. To ensure a comprehensive and up-to-date perspective, the literature included in this narrative review was identified through targeted searches in Google Scholar, PubMed, and Scopus, covering the period 2015–2025 and using keywords such as "MXene", "diabetes diagnosis", "diabetes therapy", "biosensor", "tissue regeneration", and "wound healing". Finally, we examine the challenges in clinical translation, including biocompatibility concerns, scalability, and regulatory hurdles, providing insights into future research directions for MXene applications in diabetes care.

2 MXenes in diabetes diagnostics

2.1. Importance of early detection in disease management

Early detection is a fundamental aspect of disease management that significantly improves treatment outcomes, enhances survival rates, and reduces healthcare costs. The ability to identify diseases at an early stage allows for timely intervention, which can prevent complications, minimize the severity of the condition, and increase the effectiveness of therapeutic strategies.[35] Advances in medical research and diagnostic technologies have made it possible to detect a wide range of diseases before they reach critical stages, highlighting the importance of routine screening and early diagnosis. One of the primary benefits of early detection is the improved prognosis associated with many diseases, particularly cancers and chronic conditions.[36] In addition to improving survival rates, early detection contributes to the administration of more effective and less aggressive treatments. Detecting diabetes in its early stages enables intervention strategies that can prevent complications such as neuropathy, retinopathy, and kidney damage.[37–39] Diabetes represents a significant public health concern globally,

with approximately 240 million people living with undiagnosed cases and nearly half of all adults affected unaware of their condition.[40] The disease places a heavy financial burden on healthcare systems across the world. Currently, around 537 million individuals, roughly 10.5% of adults aged 20 to 79, are managing diabetes, contributing to a global healthcare expenditure of $966 billion.[41] This economic impact is projected to rise, with costs anticipated to surpass $1054 billion by 2045. Additionally, the prevalence of diabetes continues to escalate at a concerning pace, with forecasts predicting an increase to 643 million cases (11.3%) by 2030 and 783 million cases (12.2%) by 2045. These figures underscore the critical need for better prevention strategies, timely diagnosis, and advanced monitoring tools to improve disease management.[41]

From an economic perspective, early disease detection reduces the financial burden on both healthcare systems and patients.[42] Treating diseases at an advanced stage often requires extensive medical care, prolonged hospital stays, and complex therapeutic approaches, all of which contribute to higher healthcare costs. Preventative measures, including routine screenings and early-stage treatments, are generally more cost-effective and lead to better long-term health outcomes. Moreover, early intervention reduces the need for emergency care and intensive medical procedures, leading to more efficient resource allocation within healthcare systems.[35]

Beyond medical and economic benefits, early detection has substantial psychological and emotional implications. Patients diagnosed at an early stage often experience lower levels of anxiety and uncertainty compared to those diagnosed at a more advanced stage.[43] Having early insight into a medical condition enables individuals to make well-informed choices about their treatment options and necessary lifestyle adjustments, allowing them to take greater control over their health. Furthermore, educational campaigns and awareness programs are vital in motivating people to undergo routine health assessments and screenings, promoting a preventative mindset toward disease management.[44] The importance of early detection extends across various diseases and medical conditions, reinforcing the need for continued investment in screening programs, diagnostic technologies, and public health initiatives. Routine check-ups, genetic testing, self-examinations, and wearable health monitoring devices are valuable tools in identifying diseases at their earliest stages. Focusing on early diagnosis enables healthcare systems to optimize treatment approaches, achieve better health outcomes for patients, and help alleviate the worldwide impact of disease.[45]

Within this framework, MXenes have gained attention as valuable materials for diabetes detection and management, owing to their exceptional physicochemical characteristics. Their large surface area, excellent electrical conductivity, and adaptable surface functionalities make them well-suited for use in biosensor development.[46] MXenes' excellent electrical conductivity facilitates rapid electron transfer, which enhances both the sensitivity and responsiveness of electrochemical sensing devices. Their biocompatibility and high surface functionalizing capability enable the selective detection of glucose and other diabetes-related biomarkers with enhanced specificity.[25,47] Unlike traditional enzyme-based glucose sensors, which suffer from enzyme degradation and instability, MXene-based sensors demonstrate greater durability and robustness, ensuring long-term performance. Additionally, their flexibility allows integration into wearable and implantable devices, facilitating continuous and real-time glucose monitoring with minimal patient intervention.[20] Beyond glucose sensing, MXenes have shown potential in detecting early-stage biomarkers associated with diabetes, such as insulin, C-reactive protein (CRP), and advanced glycation end-products (AGEs).[48] Early diagnosis is vital for effective diabetes prevention and management, allowing early treatment and minimizing the chances of serious complications. MXenes' capability to detect biomarkers at extremely low levels improves diagnostic precision, supporting the development of advanced point-of-care (POC) testing and personalized medicine approaches.[49]

2.2. MXene-based biosensor used for the detection of diabetes

MXenes have gained recognition as a valuable material for glucose detection and monitoring because of their distinctive and beneficial characteristics, notably their outstanding electrical conductivity, which allows for rapid and accurate detection of glucose levels, as well as biocompatibility, ensuring they are safe for long-term interaction with biological systems.[50] The extensive surface area of MXenes offers numerous active sites for interaction with glucose molecules, enhancing sensitivity and enabling the detection of even minute changes in glucose concentrations. Furthermore, their tunable surface chemistry offers the flexibility to modify their properties for optimized sensor performance. The combination of these characteristics makes MXenes particularly well-suited for integration into glucose sensing devices, enabling more efficient, reliable, and real-time monitoring for diabetes management.[51]

Glucose sensors are traditionally classified into enzymatic sensors, that are based on applying glucose oxidase (GOx) to catalyze the oxidation of glucose, and non-enzymatic types. These sensors have evolved through three generations, improving sensitivity and selectivity through the incorporation of synthetic mediators and nanomaterials. However, enzymatic sensors have some limitations such as enzyme instability, high costs, and susceptibility to environmental factors. To overcome these challenges, non-enzymatic glucose sensing devices have been designed, utilizing direct glucose oxidation at the electrode surface without the need for enzymes or mediators. MXenes, with their high surface area and excellent electron transfer properties, offer a significant advantage for non-enzymatic glucose sensing, enhancing both sensitivity and anti-interference capabilities. MXenes provide a clear advantage in this context: their high surface area, metallic conductivity, and tunable surface terminations enable efficient electron transfer and strong catalytic activity, improving both sensitivity and resistance to common interfering species. As a result, MXene-based electrodes offer a promising route toward stable, low-cost, and accurate non-enzymatic glucose sensors suitable for next-generation diabetes monitoring technologies.[52] For

instance, MXene-containing composites were used to overcome the invasive nature of blood sampling and provide more comfortable conditions for the diabetic patient. Shang *et al.* designed an innovative electrochemical sensor utilizing reduced graphene oxide (rGO)-Ti_3C_2 MXene nanocomposites for non-invasive glucose detection using saliva. The sensor was fabricated by coating a copper wire with GO-Ti_3C_2, followed by hydrothermal reduction to obtain rGO-Ti_3C_2 along with the addition of gold nanoparticles (Au NPs) to enhance its conductivity and electrocatalytic properties. A protective wax layer was applied to improve sensor stability. The Au/rGO-Ti_3C_2 electrode exhibited an extensive linear detection range between 10 μM–21 mM, and a low detection limit of 3.1 μM, underscoring its high sensitivity for glucose sensing in saliva. In here, the superior conductivity of MXene was combined with the outstanding biocompatibility of gold nanoparticles, positioning it as a promising candidate for electrochemical biosensing applications.[53]

Beyond this, MXene-based sensors could be used for real-time tracking of glucose levels without frequent invasive blood sampling. These are wearable glucose sensors integrated with MXene-based nanomaterials that exhibit more sensitivity and stability resulted from the excellent electrical conductivity, extensive surface area, and diverse surface chemistry of MXenes.[6,54] This led to the introduction of an innovative wearable biosensor used for noninvasive glucose monitoring through a novel MXene-functionalized poly(3,4-ethylenedioxythiophene) polystyrene sulfonate (PEDOT:PSS) conductive hydrogel. It was produced *via* a one-step synthesis method that combines the conductive polymer PEDOT:PSS with MXene nanosheets, resulting in a flexible and highly sensitive electrochemical sensor. The incorporation of ethylene glycol (EG), during preparation, promoted polymer chain expansion and the formation of three-dimensional porous networks, that significantly enhanced the material's electrical conductivity, mechanical flexibility, and stability. This unique composition addresses common challenges in wearable sensors, including material stacking and peeling issues often encountered with powdered components. The resulting hydrogel biosensor demonstrated exceptional performance characteristics, achieving a highly sensitive detection limit of 1.9 μM for glucose with a sensitivity of 21.7 μA mM^{-1} cm^{-2} in the physiologically relevant range of 1–94 μM. When integrated with screen-printed carbon electrodes and tested as a dermal patch, the device successfully monitored sweat glucose levels, demonstrating a high degree of agreement with traditional glucose meter measurements. The enhancement of sensor performance was related to the remarkable electron transport capabilities of MXene, which elevated the conductivity even at low concentrations (0.1% mass fraction), combined with the optimized structure of hydrogel that facilitates efficient enzyme immobilization through simple embedding.[55] This innovation marked a major step forward in wearable technology for diabetes management, providing a comfortable method for continuous monitoring that eliminates the need for invasive blood sampling. The strong correlation found between glucose levels in sweat and those in blood highlights the potential for clinical use, offering a transformative approach to how patients track their condition daily.

Another research group used sweat for non-invasive continuous monitoring of glucose *via* fabricating a 3D graphene-MXene aerogel platform *via* mixing $Ti_3C_2T_x$ MXene with reduced graphene oxide (MX-rGO) functionalized with glucose oxidase or polyaniline (PANI) that led to the production of an advanced electrochemical sensor (Fig. 1). This innovative structure greatly improved the efficiency of electron transfer between the enzyme's redox site and the electrode surface, while also ensuring stable enzyme immobilization to avoid any leakage. The system represented a major advancement in wearable diagnostics through its incorporation of an adaptive calibration mechanism that continuously monitored and compensated for sweat pH variations during physical activity. This dual-function capability addressed a critical challenge in noninvasive glucose monitoring by ensuring measurement accuracy despite natural fluctuations in sweat composition. The sensor demonstrated exceptional performance characteristics, achieving high linearity ($R^2 = 0.99$) across the physiologically relevant glucose range of 20–200 μM with a sensitivity of 15.5 μA mM^{-1} cm^{-2} and detection limit of 33.69 μM. Simultaneously, the integrated pH sensor exhibited remarkable sensitivity (62.96 mV per pH) across the biological pH range of 4–8.[56] By combining accurate glucose measurement with real-time environmental compensation, this technology enabled more dependable physiological monitoring during daily activities and exercise. It also established a foundation for developing comprehensive health monitoring systems capable of supporting personalized medicine and chronic disease management.

Biosensor patch was produced in another study incorporated with MXene/Prussian blue ($Ti_3C_2T_x$/PB) composite material, for reliable and precise monitoring of essential biomarkers such as glucose and lactate in sweat (Fig. 2A). The fabricated sensor combined the distinctive two-dimensional structure and metallic-level conductivity of MXene with Prussian blue's catalytic properties, resulting in dramatically improved electrochemical activity and stability for hydrogen peroxide detection. It was an engineered solid-liquid-air three-phase interface that guarantee unrestricted oxygen supply to the enzymatic layer, and thereby exhibited enhanced enzyme performance. This design achieved a broad linear detection range between 10×10^{-6} to 1.5×10^{-3} M, a low detection limit of about 0.33×10^{-6} M, and exceptionally high sensitivity (35.3 μA mM^{-1} cm^{-2}) for glucose detection. The platform also featured multiple sensing functions, including a pH sensor to adjust for local fluctuations that might impact measurements. In tests involving human subjects, the device effectively monitored glucose and lactate levels, simultaneously, with excellent sensitivity and consistency, surpassing the performance of prior graphene/PB and carbon nanotube/PB biosensors under practical conditions.[57]

Tear could be used as another source for the non-invasive detection of diabetic using MXene-based sensors. For example, a paper-based sensor was produced *via* deposition of few-layer nanosheets of $Ti_3C_2T_x$ onto a filter membrane followed by the addition of AuNPs. The system was further

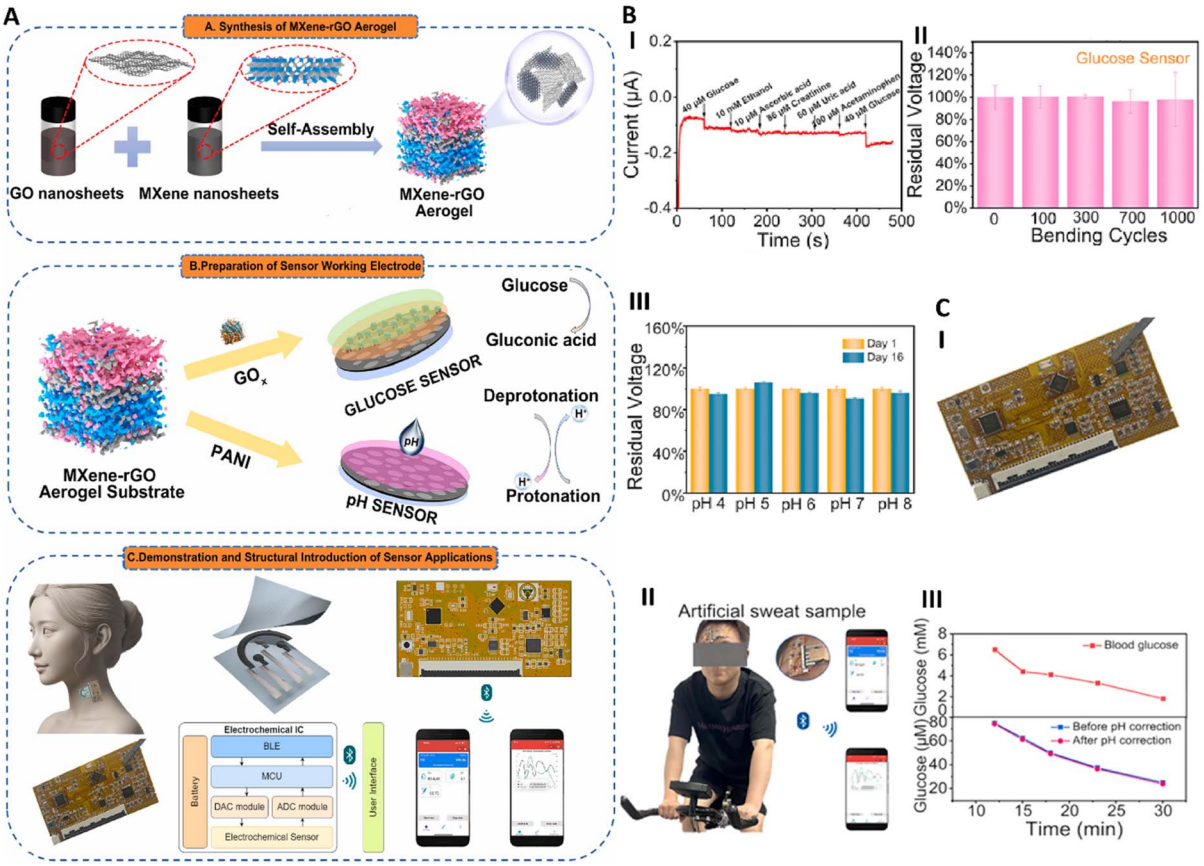

Fig. 1 (A) Schematic illustration of the biosensor fabrication process, including the formation of MXene-rGO aerogel through solvothermal self-assembly, the electrode architecture with its catalytic mechanisms for pH and glucose sensing, and the final integrated dual-functional sensor design. (B) (I) Chronoamperometric performance of the glucose sensor against common interferents. (II) Amperometric stability after varying bending durations at 100 μM glucose. (III) Long-term stability assessment of the glucose sensor. (C) (I) Photograph of the flexible printed circuit board. (II) Image of a user wearing the fully integrated bifunctional wearable sensor during cycling. (III) Real-time glucose monitoring using the forehead-mounted sensor, compared with readings from a commercial glucose meter. Reprinted with permission from ref. 56. Copyright 2024, American Chemical Society.

functionalized with GOx (Fig. 2B), which catalyzed the oxidation of glucose in tear fluid, generating hydrogen peroxide (H_2O_2). This H_2O_2 then triggered a colorimetric reaction, converting leucomalachite green (LMG) to malachite green (MG), resulting in a detectable color change. It was a type of Surface-Enhanced Raman Spectroscopy (SERS)-based sensor with improved sensitivity, resulted from the simultaneous presence of MXene and AuNPs, so that could detect very low amounts of glucose within tear fluid, demonstrating its potential as a non-invasive alternative for diabetes monitoring. The system could detect glucose at very low concentrations (as little as 0.32 μM), making it about 300 times more sensitive than typical glucose test strips. Moreover, within a linear range of 1–50 μM, the lowest detection concentration was 0.39 μM. The fabricated sensor was tested on tears of both healthy people and diabetics, which showed higher tear glucose levels in diabetic patients than in healthy individuals when fasting.[58]

MXenes have demonstrated excellent potential in capturing and detecting biomarkers due to their tunable surface properties and high adsorption capacity. They can be functionalized with antibodies or aptamers to selectively capture diabetes-related biomarkers such as glycated hemoglobin (HbA1c), insulin, and C-reactive protein (CRP). Their high surface area and electrical conductivity enhance signal transduction in biosensing applications, allowing for ultra-sensitive biomarker detection.[59,60] In this context, a new type of sensor (1D/2D KWO/$Ti_3C_2T_x$) was fabricated for the detection of acetone in breath, using potassium tungstate nanorods and $Ti_3C_2T_x$ nanosheets that showed enhancement in acetone adsorption and charge transfer. This hybrid exhibited an order-of-magnitude improvement in sensitivity over pristine KWO while operating efficiently at room temperature, a key requirement for portable diagnostics. Its resistance to humidity-induced signal drift and long-term operational stability further demonstrates the value of incorporating MXene into gas-sensing architectures. These features highlight how MXene-based heterostructures can advance low-power, miniaturized, and reliable breath acetone sensors suitable for early diabetes screening and non-invasive monitoring.[61]

An innovative electrochemical immunosensor was fabricated using a nanocomposite of AuNP and MXene for rapid, sensitive, and cost-effective detection of Cystatin C (Cys-C),

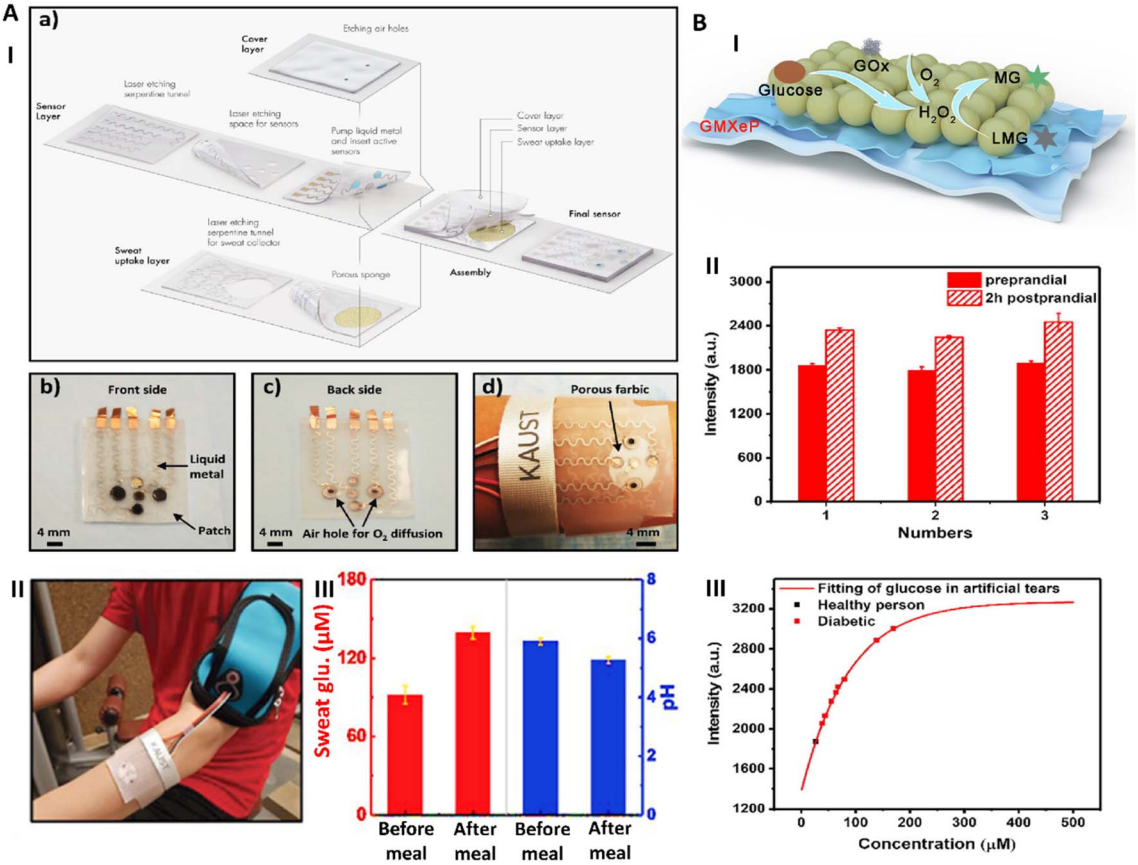

Fig. 2 (A) (I) Schematic representation and corresponding images of the wearable biosensor patch. (a) Illustration of the multilayer patch structure, consisting of a sweat-uptake layer, sensor layer, and protective cover layer. (b) Front-side optical image showing the sensor array (left and right), reference electrode (top), counter electrode (middle), and pH sensor (bottom). (c) Back-side optical image of the sensor array. (d) Optical images of the wrist-mounted sensor laminated on human skin. (II) The wearable sweat-monitoring patch connected to a portable electrochemical analyzer during on-skin operation. (III) Comparison of glucose and pH levels before and after meals measured using three different glucose and pH sensors. Reprinted with permission from ref. 57. Copyright 2019, WILEY-VCH Verlag GmbH & Co. (B) (I) Schematic of GMXeP substrate preparation and glucose detection. (II) MG SERS peak at 1613 cm^{-1} in fasting and postprandial tears of normal subjects. (III) Glucose levels in normal and diabetic tears determined from the calibration curve correlating glucose concentration with MG SERS intensity at 1613 cm^{-1}. Reprinted with permission from ref. 58. Copyright 2021, Elsevier B.V.

a critical biomarker for gestational diabetes mellitus (GDM). It was a screen-printed electrode modified with AuNPs and $Ti_3C_2T_x$ MXene *via* electrochemical deposition followed by the immobilization of papain to enable selective Cys-C binding. In clinical validation with 150 GDM patients and 150 healthy controls, serum Cys-C levels were significantly elevated in GDM patients (*e.g.*, 1.15 ± 0.26 μg mL^{-1} at 34–40 weeks *vs.* 0.97 ± 0.14 μg mL^{-1} in controls; $P < 0.05$). The sensor exhibited the linear detection range of 50–5000 ng mL^{-1} and a strong correlation with standard latex immunoturbidimetric assays ($R^2 = 0.91$). Selectivity tests showed negligible response to common interferents (including uric acid (UA), glutathione (GSH), dopamine (DA), BSA, ascorbic acid (AA), and cysteine (Cys)), and stability was maintained over 30 days with <10% signal variation. Higher levels of Cys-C were associated with a greater likelihood of negative outcomes, such as cesarean section delivery ($r = 0.304$), premature birth ($r = 0.588$), fetal distress ($r = 0.304$), postpartum hemorrhage ($r = 0.670$), and NICU admission ($r = 0.437$), all with $P < 0.05$. Therefore, the fabricated robust point-of-care biosensor presented significant potential for early risk assessment and improved management of GDM and its complications.[62]

Nucleic acids are another good target for the detection of diabetes. In this case, a highly sensitive electrochemical biosensor was designed to detect miRNA-377, a potential biomarker for diabetic nephropathy, using an innovative MXene-Au nanocomposite platform combined with a G-quadruplex nano-amplification strategy. For signal amplification, Guanine-rich DNA detection probes were conjugated to AuNPs, which form G-quadruplex structures upon target recognition. This structural change increased the binding affinity for methylene blue (MB), resulting in a 2.7-fold enhancement in electrochemical signal. The biosensor demonstrated exceptional performance, achieving a broad linear detection range from 10 aM to 100 pM and an ultra-low detection limit of 1.35 aM. The biosensor also exhibited strong selectivity and was successfully applied to detect miRNA-377 in human serum samples, confirming its potential for

clinical diagnostics.[63] This platform operated without requiring thermal cycling or reverse transcription, offering a convenient, highly sensitive, and stable alternative to conventional miRNA detection methods. The combination of MXene and Au led to superior electron transfer and the signal amplification from G-quadruplex formation made this biosensor a promising tool for early detection and monitoring of diabetic nephropathy.

In another study, a novel fluorescence resonance energy transfer (FRET) aptasensor was developed using monolayer Ti_3C_2 MXene for the simultaneous detection of insulin and visceral adipose tissue-derived serotonin (vaspin), two crucial biomarkers for diabetes diagnosis and classification. The sensor exploited the exceptional fluorescence quenching properties of Ti_3C_2 MXene, which effectively suppressed the fluorescence of fluorescein-labeled insulin-binding aptamers (IBAs) and Cy7-labeled vaspin-binding aptamers (VBAs) through FRET. When target molecules were present, insulin and vaspin preferentially bound to their respective aptamers, causing the fluorescent probes to detach from the MXene surface and restore measurable fluorescence signals. The broad-spectrum absorption capability of Ti_3C_2 enabled simultaneous quenching of both FAM (Fluorescein Amidite) and Cy7 fluorophores at different wavelengths, allowing for parallel detection of both biomarkers. The aptasensor demonstrated high sensitivity with detection limits of 36 pM for insulin and 45 pM for vaspin, along with excellent specificity in complex biological matrices. Clinical validation using human serum samples confirmed the platform's diagnostic potential for distinguishing diabetes subtypes and identifying underlying pathological causes, which could significantly improve treatment stratification.[47]

Overall, MXene-based sensors have demonstrated exceptional potential for early and non-invasive detection of diabetes biomarkers, including glucose, insulin, HbA1c, miRNAs, and tear or sweat metabolites. Their high electrical conductivity, tunable surface chemistry, and large surface area facilitate rapid electron transfer, enhanced sensitivity, and selective biomarker detection, enabling integration into wearable and implantable devices for continuous monitoring. Despite these promising features, many reported device performance metrics, such as stability, detection limits, and selectivity, are derived from single-study experiments without comprehensive evaluation of sample size (*n* values), failure rates, signal drift, or confounding factors. Consequently, the reproducibility and real-world stability of these MXene sensors remain to be systematically validated and so future research should focus on standardized, multi-center studies to verify performance claims under physiologically relevant conditions and extended operational periods, ensuring that these advanced sensors can reliably transition from laboratory prototypes to clinical and home-use applications.

Some other types of MXene-based sensors used for diabetes detection are summarized in Table 1.

3 MXenes in diabetes therapeutics

MXenes are emerging as valuable materials in biomedicine, with applications in imaging, tissue repair, sensing, cancer therapy, and drug delivery. Their properties can be improved by combining them with other materials, which makes them thicker, stronger, more uniform, and less prone to flaws. These enhancements are particularly effective in improving the electrical conductivity and electromagnetic shielding capabilities of MXenes by leveraging their magnetic properties.[95] In addition, 2D MXenes offer a range of electrical conductivities, from metallic to semiconducting, and are naturally water friendly. These traits make them suitable for drug delivery, especially when manufactured through cost-effective processes. However, their layered structure can sometimes block the formation of gaps, which might affect their magnetic and electrical behavior. This could reduce their ability to block electromagnetic interference. By integrating MXenes with conductive or magnetic materials, these challenges can be addressed, enhancing their performance in drug delivery systems.[96]

Thanks to their distinctive characteristics, such as large surface area, hydrophilic functional groups, excellent electrical conductivity, and biodegradability, MXenes have attracted significant interest in wound healing and tissue engineering applications. Researchers have integrated MXenes into various wound dressing platforms, including electrospun nanofiber membranes, hydrogels, and microneedles to harness their antibacterial effects, stimulate cell growth, and speed up tissue repair. These materials also support tissue engineering applications by enhancing angiogenesis and providing a regenerative microenvironment for effective wound healing and tissue repair.[97] MXenes have shown promising potential for treating diabetic wound healing and in tissue engineering, particularly in regenerating β-cells in the liver. MXenes could facilitate the regeneration of pancreatic β-cells, offering a potential therapeutic approach for diabetes. Their biodegradability and antibacterial properties further enhance their application in chronic wound healing associated with diabetes. Integrating MXenes into liver tissue engineering could provide a platform for regenerating β-cells, potentially improving insulin production and restoring pancreatic function.[98]

Researchers explored the use of microneedles (MNs) for diabetic wound healing, which offer advantages such as deeper drug penetration and biodegradability. For example, to overcome the mechanical strength limitations of traditional microneedles, researchers combined a poly(γ-glutamic acid) (γ-PGA)-based microneedles with Ti_2C_3 MXenes which were loaded asiaticoside (MN-MXenes-AS), a compound known to promote wound healing by enhancing epithelialization and angiogenesis (Fig. 3). MXene provided structural reinforcement through hydrogen-bond interactions with the polymer matrix and increased drug-loading capacity due to its large surface area. It was a biocompatible microneedle patch promoted angiogenesis by upregulating CD31 expression and stimulated fibroblast migration, while MXene contributed mild ROS modulation and improved tissue perfusion through its photothermal properties. *In vivo* studies in diabetic mice demonstrated that the MN-MXenes-AS treatment resulted in faster wound closure compared to controls. Furthermore, the treated wounds showed increased angiogenesis, indicated by enhanced blood vessel formation, and improved tissue regeneration,

Table 1 Some of the recent MXene-based sensors that are used for the detection of diabetes

Composite	Method of detection	Analyte	LOD	Linear range	Sensitivity	Ref.
Cu_2O/MXene/rGO ternary	Chronoamperometry (CA)	Glucose	1.1 μM	0.1–14 mM	264.52 and 137.95 μA cm^{-2} mM^{-1}	64
$Ti_3C_2T_x$ MXene/TBA/GOx	CA	Glucose	23.00 μM	0.05–0.25 0.75–27.75 μM	—	65
Ga@MXene/CS	Electrochemical detection (EC)	Glucose	0.77 μM	10–1000 μM	1.122 μA μM^{-1} cm^{-1}	66
NiO decorated PANI N assembled $Ti_3C_2T_x$ (NiOMP)	EC	Glucose	0.019 μM	5–500 μM	3551.53 μA mM^{-1} cm^{-2}	67
Cu_2O/M/AC	EC	Glucose	1.96 μM	0.004–13.3 mM and 15.3 to 28.4 mM	430.3 and 240.5 μA mM^{-1} cm^{-2}	68
$Ti_3C_2T_x$ MXene/graphene/GOx	EC	Glucose	0.10 and 0.13 mM in air-saturated and O_2-saturated PBS, respectively	0.2–5.5 mM	12.10 and 20.16 μA mM^{-1}	69
RFG/rGO/CS/GOx	EC	Glucose	79.65 μM	0–3000 μM	46.71 μA mM^{-1} cm^{-2}	70
$Ti_3C_2T_x$ MXene/PLL/GOx	EC	Glucose	2.60 μM	0.004–0.02 μM	71.42 μA mM^{-1} cm^{-2}	71
$Ti_3C_2T_x$ MXene/Cu_xO ($x = 1, 2$) (TC)	EC	Glucose	0.065 μM	1 μM–4.655 mM and 5.155–16.155 mM	361 μA mM^{-1} cm^{-2} and 133 μA mM^{-1} cm^{-2}	72
MXene-Cu_2O ($Ti_3C_2T_x$-Cu_2O)	EC	Glucose	2.83 mM	0.01–30 mM	11.061 μA^{-1} mM cm^{-2}	73
Cu/Cu_2O nanoclusters/carbon spheres (Cu/Cu_2O/CSs)	EC	Glucose	5 μM	10–690 μM and 1190–3690 μM	63.8 μA mM^{-1} cm^{-2} and 22.6 μA mM^{-1} cm^{-2}	74
TNT/GOx	EC	Glucose	8.50 μM	0.03–1.0 μM	56.60 μA mM^{-1} cm^{-2}	75
$Ti_3C_2T_x$ MXene/rGO/GOx	EC	Glucose	2.18 μM	0.005–2.5 μM	26.64 μA mM^{-1} cm^{-2}	76
GO/CS/$Ti_3C_2T_x$ MXene/GOx/SH	EC	Glucose	1.96 μM	0.0398–1.319 μM	98.10 μA mM^{-1} cm^{-2}	77
FTO-CNTs/PEI/GOx	EC	Glucose	70 μM	0.07–0.7 μM	63.38 μA mM^{-1} cm^{-2}	78
PGOx@MXene/CS	EC	Glucose enzyme	3.1 μM	0.03–16.5 mM	48.98 μA mM^{-1} cm^{-2}	79
Pt NPs/NPC@MXene/Au	EC	Glucose	7 μM	3–1500 μM	0.08268 μA mM^{-1} cm^{-2}	80
MXene/NiCo-LDH	EC	Glucose	0.53 μM	2–4096 μM	64.75 μA mM^{-1} cm^{-2}	81
Cu nanospheres@porous carbon/3D-KSCs	EC	Glucose	0.48 μM	0.15 μM–5.62 mM	0.02867 μA mM^{-1} cm^{-2}	82
Ni/LIG	EC	Glucose	0.29 μM	0.5–1666 μM	2.040 μA mM^{-1} cm^{-2}	83
GS/GNR/Ni/GCE	EC	Glucose	2.5 nM	5 nM–5 mM	2.3 μA mM^{-1} cm^{-2}	84
Copper nanowire–carbon nanotube bilayer (Cu-NW-CNT-BL)	EC	Glucose	0.33 nM	10–2000 μM	1.907 μA mM^{-1} cm^{-2}	85
Co-MOF/NF	EC	Glucose	1.3 nM	10–3000 μM	10.886 μA mM^{-1} cm^{-2}	86
ZnO/MXene	EC	Glucose	17 μM	0.05–0.7 mM	29 μA mM^{-1} cm^{-2}	87
$Ti_3C_2T_x$ MXene/graphene/AuNPs (MGA)	EC	Glucose	2 μM	2–400 μM	169.49 μA mM^{-1} cm^{-2}	88
Pt/MXene	EC	Glucose	29.15 μM	0–8 mM	3.43 μA mM^{-1} cm^{-2}	89
MXene/methylene blue	Dual-channel EC	Glucose	17.05 μM	0.08–1.25 mM	2.4 nA mM^{-1}	90
GOx/Au/MXene/Nafion	Colorimetric sensing	Glucose	5.9 μM	100–18000 μM	0.0045 μA mM^{-1} cm^{-2}	91
MWCNT/MXene/MoS_2	Field-effect transistor (FET)	Glucose	500 pM	0.01 μM–8.5 mM	1700 μA mM^{-1} cm^{-2}	92
Cu/Cu_2O/C nanoparticles and MXene-based	Quartz crystal microbalance (QCM)	Glucose	1.70 mM	3–10 mM	—	93
MXene/MoS_2	Piezotronics method	Acetone gas sensor	5.84%	5–30 ppm	—	94

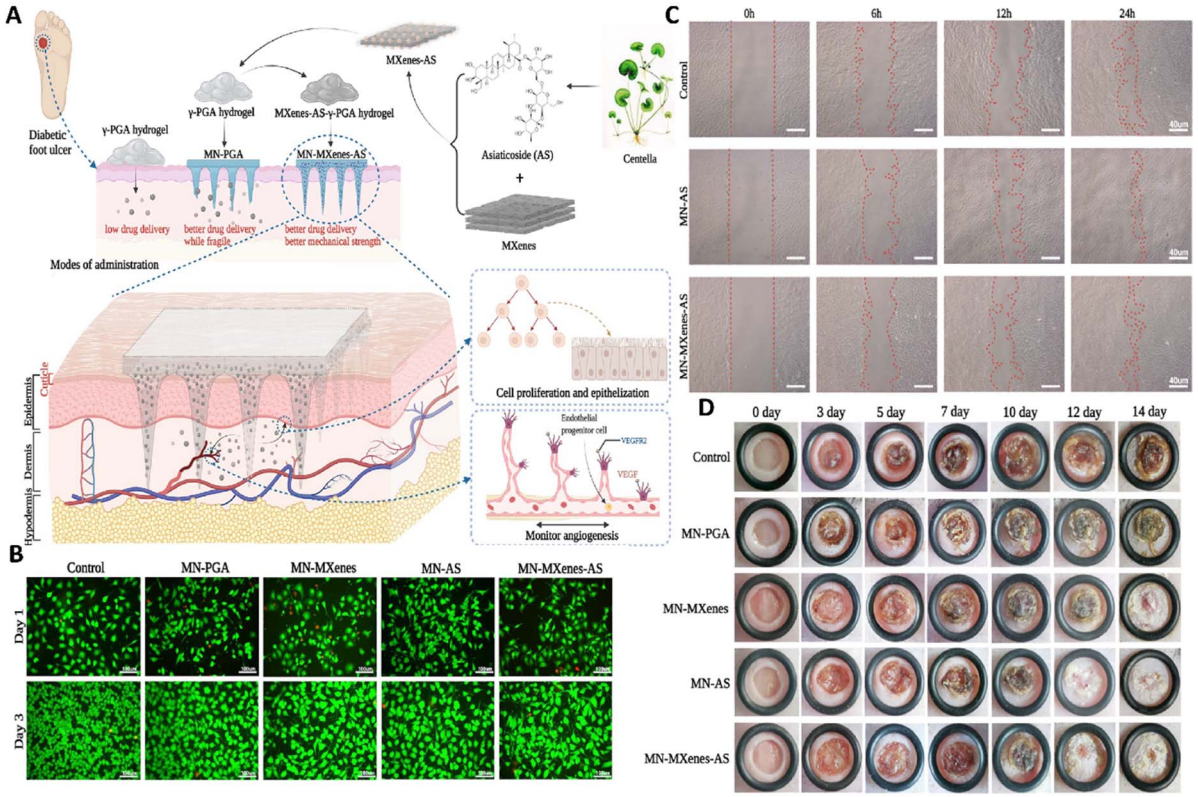

Fig. 3 (A) Diagram illustrating the MXene-based microneedle patch (MN-MOF-GO-Ag) engineered to improve the healing of diabetic wounds. (B) Confocal microscopy images of live/dead cell staining in HUVECs after co-culture with various microneedles for 24 h and 72 h. (C) Photographic images showing fibroblast migration in standard cell culture medium (control) and in medium supplemented with AS or MN-MXene-AS extract at 0, 6, 12, and 24 hours. (D) Representative images of diabetic wounds subjected to different treatments on different days. Reprinted from ref. 99 under the terms of the Creative Commons CC BY license. Copyright 2022, Springer Nature.

resulting in better healing outcomes.[99] According to the results of this study, MXenes not only could enhance the mechanical strength of microneedles but also induce sustainability in drug release pattern that led to the enhancement in therapeutic performance.

A γ-PGA-based microneedle (MN) patch incorporating GOx-loaded Ti_3C_2 MXene nanosheets (MN-PGA-MXene-GOx) was developed to address the glucose-rich, highly inflamed milieu of diabetic wounds. In this design, the MN array enabled GOx to penetrate deeply into the tissue, where the enzyme converted excess glucose into gluconic acid, effectively lowering local glucose levels and re-acidifying the wound bed. The Ti_3C_2 MXene component not only acted as a reservoir for controlled GOx release but also functioned as a mild photothermal agent; upon near-infrared (NIR) exposure, it produced gentle heating (~40 °C) that enhanced enzymatic activity, enhancing perfusion, and supported angiogenic and proliferative processes. Both γ-PGA and MXene further helped counter oxidative stress by quenching reactive oxygen species (ROS), including hydrogen peroxide produced during glucose metabolism. In diabetic mouse studies, application of the MN-PGA-MXene-GOx patch led to markedly faster healing, attenuated inflammation, and elevated collagen formation and vascular growth. Tissue examinations revealed robust granulation, improved epithelial regeneration, and upregulated vascular markers. The therapeutic benefits stemmed from the coordinated actions of glucose depletion, ROS modulation, and MXene-mediated photothermal stimulation, collectively shifting the wound microenvironment toward regeneration. NIR-triggered heating also encouraged endothelial migration and supported better microcirculation. Safety assessments showed good compatibility with blood and tissue, with no notable immune-related toxicity.[100]

The Fe_3O_4/MXene (FM) heterojunction-laden loaded into the double-layer gelatin methacryloyl (GelMA) microneedle (GFM) were used for treating infected diabetic wounds. Incorporation of $Ti_3C_2T_x$ MXene provided strong NIR related photothermal responsiveness, allowing rapid heat generation to stoped the bacterial growth and simultaneously enhanced the catalytic performance of the FM hybrid. The FM nanozyme exhibited catalase (CAT)- and superoxide dismutase (SOD)-like activities, helping modulate excessive ROS in injured tissue. Additionally, the controlled release of Fe^{2+}/Fe^{3+} ions induced bacterial ferroptosis by elevating intracellular ROS and triggering lipid peroxidation, ultimately compromising bacterial membranes and effectively eliminating *Escherichia coli* (*E. coli*), *Staphylococcus aureus* (*S. aureus*), and methicillin-resistant *Staphylococcus aureus* (MRSA). *In vivo* studies using a diabetic rat model

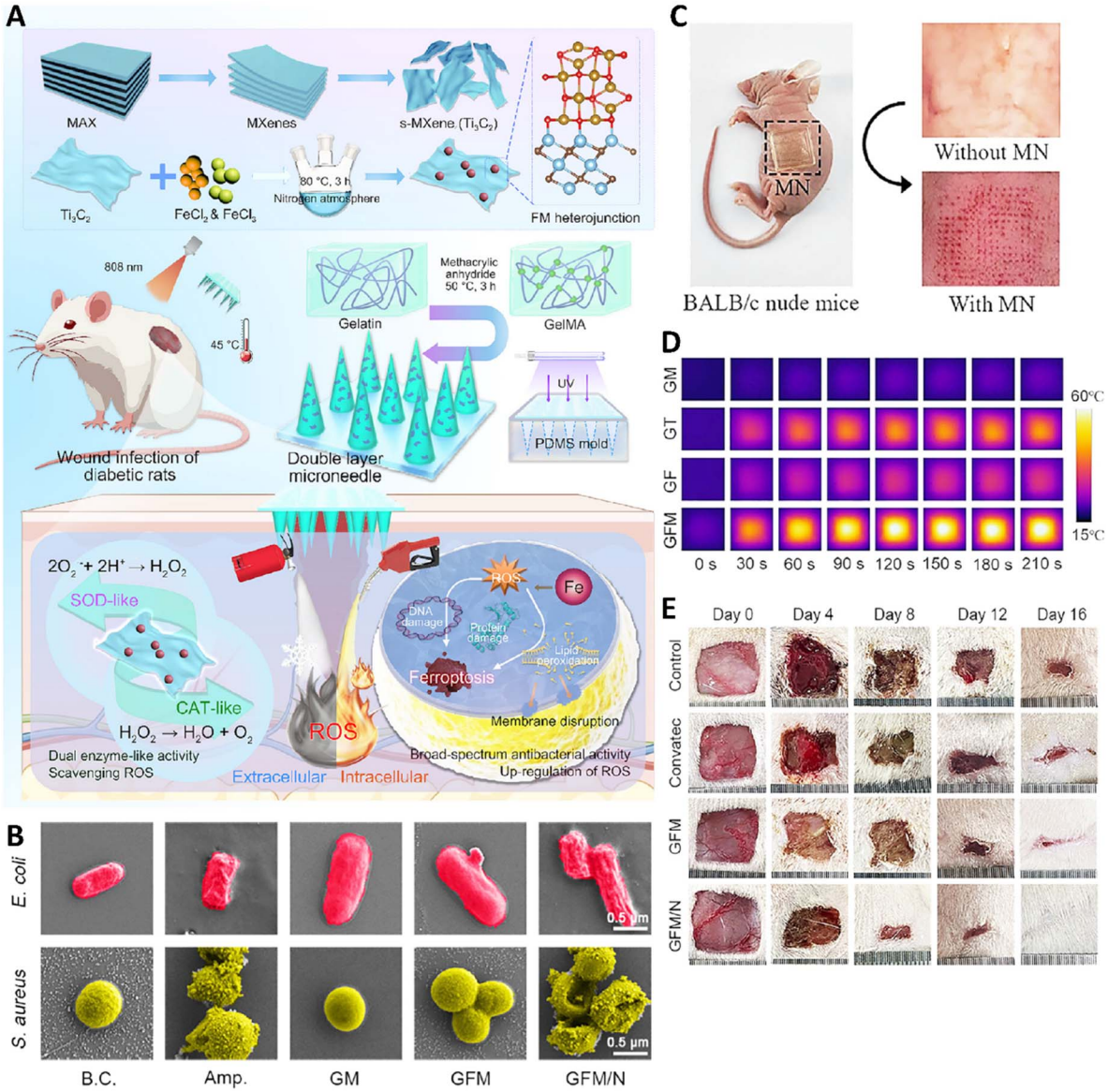

Fig. 4 (A) Illustration depicting the fabrication steps and therapeutic use of the double-layer microneedle integrated with the FM heterojunction for biomedical applications. (B) SEM images showing bacterial morphology. (C) GFM microneedle inserted into the skin of BALB/c nude mice. (D) *In vitro* photothermal conversion performance of the microneedles. (E) Optical images depicting wound sites. Reprinted from ref. 101 under the terms of the Creative Commons CC BY license. Copyright 2025, Wiley.

showed that the GFM microneedle significantly accelerated wound closure, reduced inflammation, and enhanced collagen deposition and angiogenesis, surpassing the efficacy of commercial wound dressings. Histology further confirmed improved re-epithelialization and vigorous neovascular formation, and biocompatibility evaluations showed low toxicity and good hemocompatibility (Fig. 4).[101]

Besides microneedles, MXenes were also used in the structure of hydrogels and were used to address the challenges of diabetic bone defect healing. For example, a multifunctional hydrogel was produced *via* combining copper-functionalized MXene nanosheets with GelMA and alginate-*graft*-dopamine (Alg-DA). The system exhibited photothermal therapy (PTT) effect and controlled release of Cu^{2+} ion, in response to the NIR light irradiation and pH changes. The strong photothermal conversion ability of MXene led to a significant antibacterial activity and enhanced angiogenesis and osteogenesis by improving blood circulation and cellular activity. Furthermore, MXene enabled the controlled release of Cu^{2+} ions in a pH-responsive manner, ensuring a sustained effect on reducing oxidative stress, modulating immune responses (*via* promoting macrophage polarization toward the M2 phenotype), and so promoting tissue regeneration. It also promoted adhesion, migration, and proliferation of bone-forming cells while inhibiting osteoclast activity, thereby preventing bone resorption and ensuring balanced bone repair. In diabetic rat models with critical-sized cranial defects, the fabricated hydrogel not only enhanced vascularization and bone regeneration but also

accelerated wound healing by reducing oxidative stress and creating a favorable immune environment.[102] Therefore, the photothermal feature of MXenes could lead to inducing antibacterial activity and promote tissue repair and regeneration, that introduce them as a good candidate for treating diabetic related disease.

In another research, a multifunctional implant was fabricated using a bio-heterojunction enzyme coating the combination of tantalum carbide MXene (Ta_4C_3 MXene), silver phosphate (Ag_3PO_4), and glucose oxidase (GOx) to control diabetic implant-associated infections. In here, MXene acted as the primary electron-transfer mediator, enabling efficient NIR photothermal conversion and enhancing charge separation at the Ta_4C_3/Ag_3PO_4 interface. This improved catalytic efficiency supported a cascade of ROS-generating reactions, including GOx-produced hydrogen peroxide (H_2O_2) feeding Ag_3PO_4-driven Fenton-like and laccase-mimicking pathways. MXene simultaneously depleted intracellular glutathione (GSH), weakening bacterial antioxidant defenses and increasing susceptibility to oxidative damage. These combined photothermal and catalytic mechanisms disrupted biofilms and produced broad-spectrum antibacterial activity, while the MXene-modified surface also supported osteogenic responses by improving cell adhesion and proliferation, and calcium nodule formation. In diabetic infection models, the implant reduced inflammation, enhanced collagen deposition, and improved tissue regeneration (Fig. 5A–C).[103]

The photothermal capability of MXenes was used in another research to produce a composite wound dressing mat composed of microgels containing titanium carbide MXene (Ti_3C_2 MXene) nanosheets incorporated into the chitosan/gelatin matrix nanofibers (Fig. 5D). The fabricated formulation showed dual photothermal properties; high-temperature PTT, which was related to the presence of chitosan/gelatin matrix and led to the rapid bacterial eradication and biofilm disruption and so, sterilizing the composite, and mild heating (MPTT), which was provided by MXene microgels and led to the promotion of fibroblast migration and tissue regeneration. In this formulation, presence of chitosan/gelatin matrix provided biocompatibility, structural integrity, and moisture retention, ensuring a stable and conducive healing environment, while the MXene part showed potential in stimulating cellular responses essential for tissue repair, making the system effective for both infection control and the promotion of diabetic wound healing. *In vivo* tests confirmed that the dressing not only combated infection but also significantly accelerated the healing process by enhancing vascularization and tissue regeneration *via* supporting the proliferation and migration of fibroblasts.[104]

$Cu_2O/Ti_3C_2T_x$ nanocomposite was developed in another study to address the impaired wound healing commonly

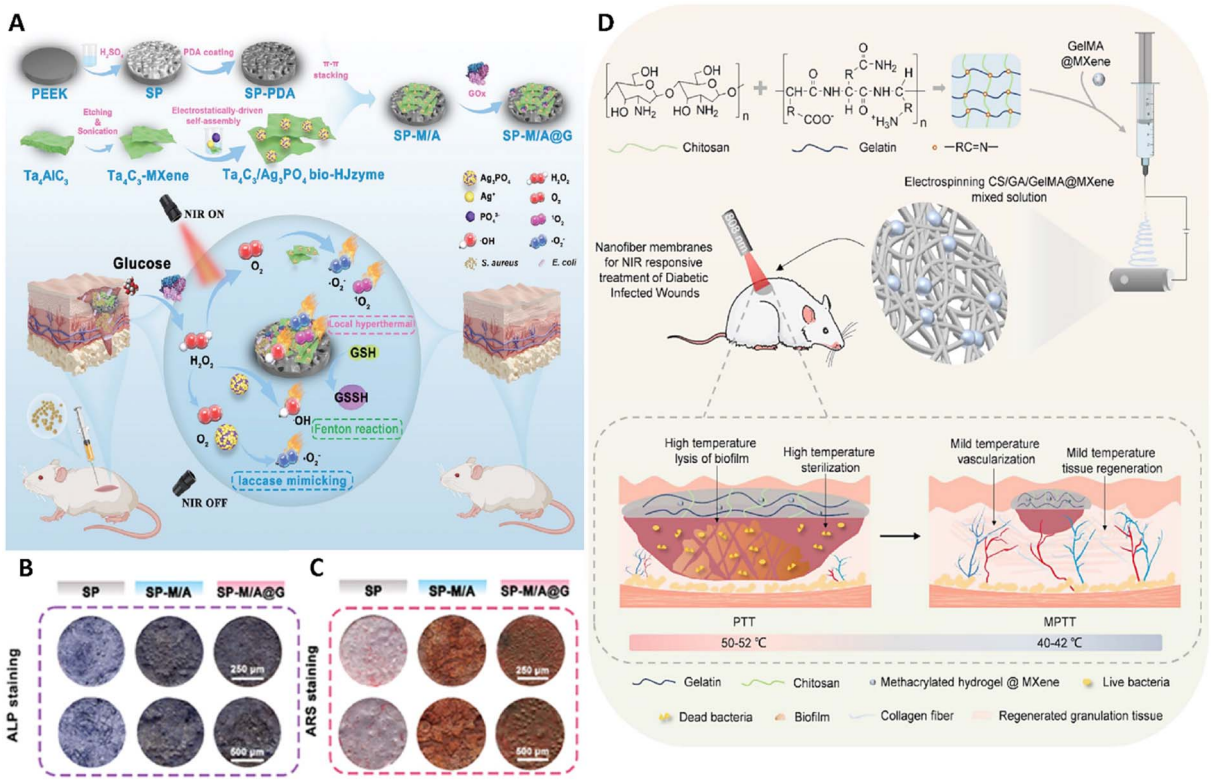

Fig. 5 (A) Schematic illustrating the fabrication process of SP-M/A@G and its cascade-amplified therapeutic mechanism for treating implant-associated infections. (B) Alkaline phosphatase (ALP) staining results ($n = 3$ per sample). (C) Alizarin Red S (ARS) staining results, ($n = 3$ per sample). Reprinted with permission from ref. 103. Copyright 2025, Wiley-VCH GmbH. (D) Diagram depicting the production of membrane dressings *via* electrospinning, incorporating MXene-loaded microgels within a chitosan/gelatin polymer matrix to enhance the healing of infected diabetic wounds. Reprinted from ref. 104 under the terms of the Creative Commons CC BY license. Copyright 2024, Springer Nature.

observed in diabetic patients, particularly when complicated by infections from multidrug-resistant bacteria such as MRSA. This nanocomposite exhibited minimal cytotoxicity toward NIH-3T3 fibroblast cells at concentrations up to 50 μg mL^{-1}, even after NIR irradiation, indicating their biocompatibility. It also demonstrated excellent stability with low metal ion leaching and negligible hemolytic activity at concentrations up to 400 μg mL^{-1}. *In vivo* studies using MRSA-infected diabetic mice revealed that topical application of $Cu_2O/Ti_3C_2T_x$ nanosheets, coupled with NIR irradiation, significantly reduced wound area and bacterial load. The enhanced antimicrobial effect was linked to the photothermal response and ROS production, which disrupted bacterial membranes and promoted bacterial eradication. Histological analyses of treated wounds revealed increased collagen deposition, enhanced angiogenesis, and improved epithelialization, all of which are essential for effective tissue repair in diabetes-related chronic wounds.[105] According to the results of this research, MXenes could not only be used against normal bacteria, but also, they could affect antibiotic resistance form of bacteria and could be effectively used against chronic wounds such as diabetic foot ulcers.

An innovative sponge scaffold was fabricated for diabetic wound management by integrating hydroxypropyl chitosan (HPCS) and porcine acellular dermal matrix (PADM) with Ti_3C_2Tx (MXene) nanosheets. The fabricated scaffold demonstrated robust antibacterial activity, eliminating 98.89% of *S. aureus* and 97.21% of *E. coli* within 36 h. It also demonstrated excellent biocompatibility, showing no cytotoxic effects on human umbilical vein endothelial cells (HUVECs) or mouse fibroblasts (L929 cells), while significantly enhancing cell proliferation, migration, and angiogenesis. In diabetic rat models, the K1P6@Mxene scaffold reduced inflammation, enhanced collagen deposition, and accelerated wound healing by seven days compared to the controls. Histological analysis revealed improved re-epithelialization, angiogenesis, and minimal scarring, underscoring the scaffold's potential as a multifunctional material for diabetic wound care. By contributing to the scaffold's electrical conductivity, MXenes enabled effective coupling with the endogenous electric fields present at wound sites. This coupling facilitated directed cell migration and proliferation, both of which are crucial for effective tissue regeneration. Moreover, the photothermal properties of MXenes allowed for the absorption of NIR light, leading to localized heating that can further enhance antibacterial efficacy and promote tissue repair processes. Collectively, these attributes made the fabricated MXene-integrated scaffolds a promising approach for improving diabetic wound healing outcomes.[106]

To prevent diabetes-related biofilm infections (DRBIs), a DNase-I-loaded vanadium carbide MXene (DNase-I@V_2C) nanoregulator was developed by combining the enzymatic activity of DNase-I with the antioxidant and biofilm-penetration properties of V_2C MXene. This system degraded extracellular polymeric substances (EPS) and neutrophil extracellular traps (NETs) in biofilms, allowing the immune system to combat infections more effectively. Additionally, the nanoregulator redirected neutrophil activity from NETosis to phagocytosis by scavenging ROSs and modulating immune signaling pathways. DNase-I@V_2C exhibited strong SOD- and CAT-like activity, effectively degrading biofilms by reducing EPS integrity and biomass, while preserving DNase-I activity. It suppressed NET formation, enhanced phagocytosis, and facilitated efficient bacterial clearance. In diabetic rat models, the nanoregulator accelerated biofilm clearance, reduced bacterial loads, and promoted tissue regeneration in infected joints. It also improved healing of wound *via* inducing epidermal growth, angiogenesis, and collagen deposition, resulting in faster wound closure and improved dermal reconstruction.[107]

Interestingly, MXenes, in combination with other compounds, could appear in the role of an immunoregulator agent and help in treating diabetic wounds *via* engineering the immune system. For example, to overcome the barriers in the recovery of diabetic ulcers, a bioactive hydrogel composite (FM-Exo hydrogel) was developed *via* integrating M2 macrophage-derived exosomes (M2 macrophage-derived extracellular vesicles) and MXene (F127-functionalized titanium carbide nanosheets). MXene provided antibacterial activity and enhanced exosome retention, while the exosomes delivered anti-inflammatory and pro-regenerative signals. Indeed, MXene stabilized the exosomes and modulated macrophage behavior, while sustained exosome release activated the phosphoinositide 3-kinase/protein kinase B (PI3K/AKT) pathway, driving M1 → M2 polarization. This shift suppressed tumor necrosis factor (TNF-α) and increased vascular endothelial growth factor (VEGF) secretion, creating a microenvironment that supported fibroblast proliferation, endothelial migration, and angiogenesis. The system also restored cell activity that was disrupted under high glucose, largely through macrophage-mediated paracrine signaling. *In vivo* tests showed that FM-Exo reduced inflammation, increased M2 macrophage abundance, enhanced neovascularization, and promoted organized collagen deposition (Fig. 6).[108]

Besides healing wounds or other types of diabetic related disease, MXenes could be used for treating diabetes itself, using stem cells. For example, an innovative 3D culture system was designed using Ti_2C MXene composite nanofibers to address the challenges of pancreatic β-cell generation for diabetes therapy. These nanofibers were fabricated by doping polycaprolactone (PCL) with Ti_2C nanosheets through an electrospinning process, resulting in a scaffold with enhanced porosity, hydrophilicity, and cytocompatibility. The incorporation of MXene into nanofiber scaffolds created a favorable microenvironment that supported the adhesion, growth, and lineage-specific differentiation of human Wharton's jelly-derived mesenchymal stem cells (hWJ-MSCs) toward pancreatic β-cell phenotypes. The differentiation process was evaluated through the expression of essential β-cell transcription factors and proteins such as Pancreatic and Duodenal Homeobox 1 (PDX-1), MAFA, and insulin, alongside functional assessments including glucose-stimulated insulin secretion (GSIS). Compared to polycaprolactone (PCL) nanofiber controls, the Ti_2C-enhanced scaffolds notably enhanced stem cell attachment, proliferation, and pancreatic differentiation. Cells cultured on these MXene-enriched nanofibers showed elevated

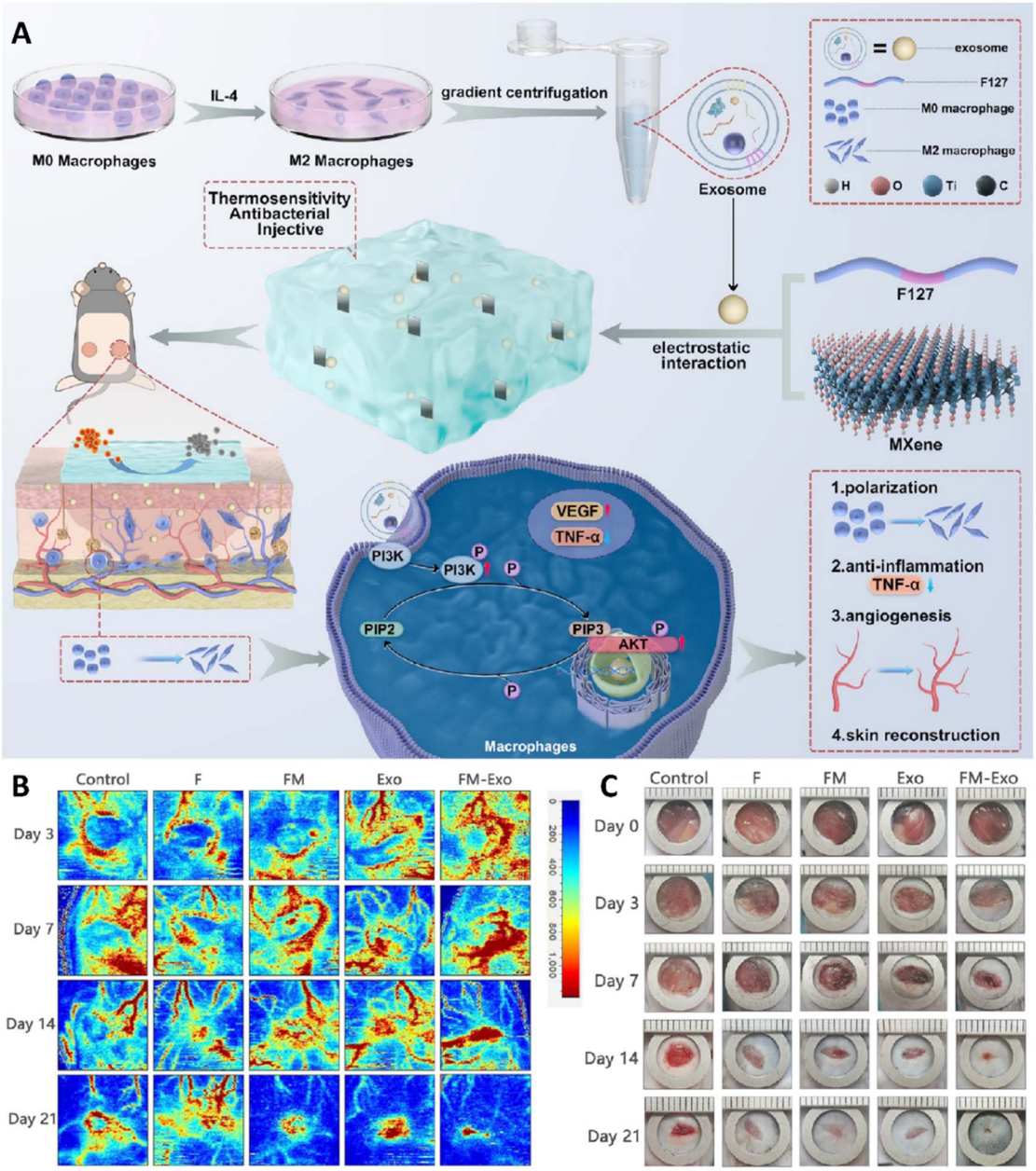

Fig. 6 (A) Schematic representation of the FM-Exo hydrogel, showcasing its multifunctional properties for diabetic wound healing and skin regeneration. (B) Laser doppler images depicting subcutaneous vascular flow and blood supply in the wound area. (C) Sequential wound images illustrating the healing process over time. Reprinted with permission from ref. 108. Copyright 2024, American Chemical Society.

expression levels of β-cell marker and demonstrated enhanced insulin secretion in response to glucose challenge, confirming the scaffold's effectiveness in promoting functional islet-like cell development. Besides, low levels of cytotoxicity and oxidative stress confirmed the biocompatible nature of the material.[109] Therefore, these nanofibers enhanced stem cell adhesion, proliferation, and differentiation, showing higher β-cell marker expression and insulin secretion, making them a strong candidate for advancing stem cell-based treatments.

Table 2 summarizes recent advances in MXene-based composite materials developed for diabetes therapy. These composites integrate MXene nanosheets with various functional components to enhance therapeutic efficacy through improved biocompatibility, targeted drug delivery, reactive oxygen species (ROS) scavenging, antibacterial properties, and electrical conductivity. The multifunctional properties of these MXene Composites have demonstrated encouraging outcomes in speeding up the wound healing process, regulating oxidative stress, and promoting tissue regeneration in diabetic models.

4 Challenges

4.1. Synthesis and scalability

One of the foremost challenges in the application of MXenes is their complex and hazardous synthesis process. MXenes are typically produced by selectively etching the "A" layers from

Table 2 Some of the recent MXene-based composites have been used for diabetes therapy

Composite	Type of MXene	Therapeutic effect	Results	Ref.
TM-mRNA/MXene/HA microneedle hydrogel	$Ti_3C_2T_x$	Angiogenesis ↑; endothelial migration ↑; PTT-responsive release	Regeneration ↑; collagen deposition ↑; superior wound closure *vs.* IV/ID delivery	110
MXene-PDA (PMAg)/P(AM-*co*-SBMA) E-skin	$Ti_3C_2T_x$	Electrical stimulation-enhanced healing; motion/health sensing	High-sensitivity motion/physiological sensing; reliable signals; supports diabetic wound healing	111
GOx-CeO_2@MXene quantum-dot bio-HJ	$Ti_3C_2T_x$	POD/CAT-like catalysis; glucose ↓; $^{\bullet}OH$ ↑; inflammation ↓	99.99% antibacterial (*E. coli*, *S. aureus*); angiogenesis ↑; faster wound closure; inflammation ↓	112
MXene@TiO_2-GA/OKGM hydrogel	MXene@TiO_2	PTT antibacterial; ROS scavenging; ES-induced fibroblast proliferation, collagen ↑, angiogenesis ↑	Hemostasis ↑; antibacterial; accelerated healing; inflammation ↓; proliferation ↑; safe	113
MXene-TA/PEGDA-gelatin scaffold (PGMT)	Ti_3C_2	ROS scavenging; inflammation ↓; ES-driven proliferation & regeneration	ROS removal ↑; wound healing ↑; faster closure; angiogenesis ↑ with ES	114
KC/PF-TA hydrogel + MXene-Ag NPs	$Ti_3C_2T_x$	PTT antibacterial; anti-inflammatory; angiogenesis ↑; regeneration ↑	Cell proliferation/migration ↑; healing ↑ in infected diabetic wounds; antibacterial; anti-inflammatory; regenerative	115
HA-DA + PDA/MXene hydrogel	Ti_3C_2	O_2 ↑; ROS ↓; antibacterial; anti-inflammatory; PTT; regeneration ↑	O_2 delivery ↑; ROS ↓; infection inhibition; M1 → M2 shift; endothelial growth ↑; accelerated healing with mild PTT	116
MXene-magnetic colloids/PNIPAM-alginate DN hydrogel	$Ti_3C_2T_x$	Photo-magnetic release; toxicity ↓; healing ↑	Stimuli-responsive drug release; improved healing of full-thickness infected wounds	117
MXene-GelMA-TA hydrogel	$Ti_3C_2T_x$	E/ROS regulation; antioxidant; fibroblast ↑; inflammation ↓; angiogenesis ↑; collagen ↑	Fibroblast protection; ROS ↓; function restored; healing ↑ (conductivity + ROS control)	118

MAX phases (ternary carbides or nitrides) using strong acids, most commonly hydrofluoric acid (HF) or HF-containing mixtures. This etching process is not only highly corrosive and toxic, posing significant safety risks to researchers and manufacturing personnel, but also environmentally unfriendly. The use of HF requires stringent handling protocols and waste management systems, which increase production costs and complicate scaling up for industrial or clinical applications. Furthermore, the synthesis involves multiple steps such as etching, washing, delamination, and purification to obtain high-quality MXene nanosheets. Each step affects the yield, purity, and reproducibility of the final product. Achieving consistent batch-to-batch quality is challenging, which is critical for biomedical applications where material uniformity impacts sensor performance and therapeutic efficacy. The current laboratory-scale methods are not easily scalable, and there is a pressing need for safer, cost-effective, and scalable synthesis routes that can produce MXenes with controlled size, morphology, and surface chemistry.[119,120]

4.2. Stability and oxidation issues

MXenes are intrinsically prone to oxidation and structural degradation when exposed to air, moisture, or biological fluids, leading to the formation of surface metal oxides that diminish electrical conductivity, mechanical integrity, and catalytic performance. This instability limits their shelf life and complicates their use in biosensors and implantable systems for diabetes monitoring. Recent studies have introduced improved oxidative-stabilization strategies, including polyphenol-based surface passivation (*e.g.*, tannic acid, catechol derivatives) that scavenge radicals and anchor robust antioxidant layers onto MXene surfaces.[121–123] These coatings not only slow edge-initiated oxidation but also provide functional handles for grafting polymer brushes. Parallel efforts using covalent crosslinking chemistries, such as silane, epoxide, and borate linkers, have enabled the formation of protective hybrid networks around MXene sheets while maintaining electrical pathways, significantly prolonging conductivity retention in aqueous and physiologic environments.[124–128] Several reports

further demonstrate the integration of stabilized MXenes into flexible sensor films and hydrogel scaffolds with greatly enhanced ambient and aqueous lifetimes.[129–133] Despite these advances, most stabilization studies still focus on short-term performance (days to weeks) and emphasize material properties rather than long-term oxidation kinetics in serum or interstitial fluid. Therefore, standardized, biologically relevant degradation assays remain critically needed to translate stabilized MXenes into reliable clinical biosensing platforms.

4.3. Biocompatibility and long-term toxicity concerns

While MXenes show promising biocompatibility in preliminary studies, comprehensive long-term biocompatibility and toxicity evaluations are still lacking.[134] Emerging studies indicate that chronic exposure to MXenes can activate subtle immune pathways, including macrophage polarization, delayed cytokine release, and inflammasome modulation, depending on size, surface terminations, oxidation state, and concentration.[135–137] Biodistribution reports show transient accumulation in organs such as the liver, spleen, and kidneys, yet long-term clearance pathways and the fate of degradation products remain poorly defined. These concerns are particularly relevant for diabetes-related applications that require prolonged or repeated exposure, such as continuous glucose monitoring implants, chronic wound dressings, or long-acting drug delivery systems.[137,138] Moreover, MXene degradation under physiologic oxygenation is a critical factor for clinical translation. Exposure to oxygenated biological fluids can lead to oxidation of MXenes, producing metal oxide byproducts that may influence cytotoxicity, immune responses, and *in vivo* stability. $Ti_3C_2T_x$, for instance, undergoes rapid oxidation and hydrolytic degradation in aqueous, oxygen-rich environments, generating TiO_2 nanoparticles and carbide-derived carbon fragments. These byproducts can alter biological interactions and may induce oxidative stress or membrane damage at elevated concentrations.[139–141] A recent *in vivo* study showed that MXene-based biomaterials endowed with magnetoelectric and bioactive functionality were capable of actively regulating macrophage behavior: the material facilitated an initial M1 response (helpful for bacterial clearance) followed by a switch to M2 polarization, thereby promoting wound healing and inflammation resolution in infected tissue.[142] This provides one of the few direct demonstrations that MXenes can modulate immune responses beyond passive biocompatibility. While these results are promising, the study remains the exception rather than the rule, comprehensive long-term immunology evaluations, fibrosis assessment, and systemic clearance studies are still missing. Fibrotic foreign-body responses after implantation are a major translational concern for any long-term device, but data on fibrosis specifically caused by MXenes are extremely limited. While animal studies of MXene-containing wound dressings have shown favorable healing outcomes with little acute histopathological toxicity, these studies typically follow animals for days to a few weeks and do not assess chronic fibrosis or late-stage extracellular matrix remodeling around implanted materials. While initial studies suggest that surface functionalization can overcome these effects, a comprehensive analytical evaluation of degradation kinetics and toxicity under physiologic oxygenation remains lacking, representing an important area for future research. Regulatory approval for clinical use requires extensive *in vivo* safety data, which is currently insufficient. Developing standardized protocols for toxicity assessment and understanding the degradation products of MXenes in biological environments are critical steps to ensure patient safety.[143–146]

4.4. Reproducibility, standardization, and regulatory barriers

For MXene-based platforms to be adopted in clinical settings, reproducibility and standardization of material properties and device performance are essential. Variations in synthesis parameters, including precursor purity, etching conditions, delamination yield, and storage environments, can produce significant batch-to-batch inconsistencies, affecting flake size, surface chemistry, oxidation state, and electrical performance, which in turn influence sensor sensitivity, specificity, and therapeutic outcomes. These variations pose a major barrier to reliable device manufacturing.[147,148] In addition to material reproducibility, regulatory and translational barriers remain substantial. Conventional sterilization methods (*e.g.*, autoclaving, gamma irradiation, or ethylene oxide exposure) are often incompatible with MXenes: recent work demonstrated that standard sterilization processes can accelerate oxidation or alter surface terminations, leading to degradation of electrical and structural properties in devices made from $Ti_3C_2T_x$ MXene.[148,149] Without validated, MXene-compatible sterilization protocols, achieving sterility while preserving material function is difficult, a critical step for any biomedical implant or diagnostic device. Moreover, formal regulatory frameworks (*e.g.*, ISO/ASTM standards for nanomaterial characterization, sterility assurance, and biocompatibility testing) are not yet fully established for 2D materials like MXenes. As noted in recent comprehensive reviews, the absence of agreed-upon guidelines for quality control, long-term stability testing, and batch certification complicates translation of MXene platforms from lab research to clinical use. To overcome these hurdles, coordinated efforts are required to define robust, industry-wide standards and harmonized manufacturing/characterization procedures, including traceable synthesis protocols, QC metrics (flake size distribution, surface chemistry, oxidation level), sterility validation, and stability assays under physiological conditions.[150]

4.5. Integration with existing technologies

While MXenes exhibit excellent properties for biosensing and wound healing, integrating them with existing diagnostic platforms and therapeutic devices can be challenging.[151–153] Issues such as material compatibility, device fabrication complexity, and scalability need to be addressed. For instance, incorporating MXenes into flexible, wearable sensors requires ensuring mechanical durability and stable electrical contacts under physiological conditions.[154] Similarly, MXene-based wound

dressings or patches must be designed to provide controlled drug release, biocompatibility, and ease of application, which demands interdisciplinary collaboration between materials scientists, bioengineers, and clinicians.[34]

4.6. Cost and commercial viability

The current production costs of MXenes are relatively high due to expensive precursors, hazardous chemicals, and complex synthesis procedures. This limits their commercial viability, especially for widespread use in resource-limited settings where diabetes prevalence is high. To make MXene-based diagnostics and therapeutics accessible, cost-effective manufacturing processes and supply chains must be developed.[120]

4.7. Clinical translation challenges

Clinical trials are essential for translating laboratory findings into practical clinical use. While preclinical studies provide foundational knowledge about safety, efficacy, and mechanisms of action, they often fail to account for the complexities of human physiology and variability in patient populations.[155] For example, a therapeutic system might perform exceptionally well in controlled laboratory settings but yield unexpected side effects or reduced efficacy when applied in a diverse clinical setting.[156] Clinical trials ensure these potential gaps are addressed by testing interventions under rigorous, standardized conditions across varied populations.[156]

Translating advanced therapeutics to clinics also involves addressing regulatory and ethical considerations. Regulatory bodies, such as the FDA or EMA, require extensive clinical data to evaluate whether a novel therapy meets the standards for patient safety and efficacy. This includes long-term monitoring for potential adverse effects and validation of manufacturing processes to ensure consistency. Clinical trials provide the necessary evidence to support these evaluations and build the trust of both regulators and healthcare providers. Furthermore, clinical trials help establish the therapeutics' real-world value. By comparing new therapies with existing standards of care, trials identify not only the clinical benefits but also the cost-effectiveness and patient outcomes, critical factors influencing adoption in healthcare systems. Without these trials, promising technologies risk remaining confined to research settings, unable to make meaningful impacts on patient care. This highlights the essential role of clinical trials in ensuring that innovations reach their intended beneficiaries safely and effectively.[157]

MXene-based technologies show great promise as therapeutic and diagnostic tools, especially for treating the complex health needs of diabetic patients. Applications like drug delivery and wound healing are exciting, but moving these technologies into real-world medical use requires thorough clinical trials. These trials are vital to check the safety, compatibility with the human body, how they work over time, and any long-term effects.[158] Diabetic patients have unique challenges, such as slower wound healing, weaker immune systems, and higher risks of infections and other complications.[159] Treatments must be carefully designed and tested to avoid making these problems worse. Clinical trials help find the best doses, delivery methods, and how MXene-based systems interact with the body to make sure they are safe and effective for everyone, including diabetic patients. These trials are also important for meeting regulatory standards and getting approval from organizations like the FDA.[157] They build confidence in the safety and usefulness of MXene technologies for doctors and patients. By comparing MXene treatments with existing options, these trials can show if they provide faster healing, better drug delivery, or fewer side effects. Additionally, clinical trials help us understand how different patients respond to MXene-based treatments. This is especially important for diabetes, where each patient's condition can be very different. Testing ensures that treatments can be personalized to meet individual needs. Overall, these trials are essential to make sure MXene-based technologies are safe, reliable, and effective for improving patient care.[155]

5 Future perspectives

The landscape of diabetes management is poised for a paradigm shift, driven by the integration of MXene-based composites with cutting-edge technologies.

5.1. Artificial intelligence (AI) and machine learning (ML)

AI and ML technologies are poised to transform MXene-based biosensing platforms for diabetes management by enabling real-time, high-accuracy interpretation of complex physiological data. When paired with MXene sensors, known for their high conductivity, sensitivity, and multimodal signal capture, AI models can detect subtle glucose fluctuations, predict metabolic trends, and even identify early indicators of diabetic complications before clinical symptoms appear. This synergy promises personalized, continuous, and high-fidelity monitoring for both diagnostic and therapeutic applications. To fully realize the potential of AI-assisted MXene biosensing, future work must adopt standardized datasets, open-source benchmarking protocols, and robust model validation across diverse physiological conditions. Privacy protection, algorithmic transparency, and integration of materials-specific factors, such as MXene degradation, surface terminations, and batch-to-batch variability, into ML pipelines are also essential steps toward reliable, clinically deployable systems.

5.2. Novel drug delivery systems

Innovations in drug delivery are also gaining momentum. MXenes' excellent electrical conductivity, flexibility, and biocompatibility make them ideal for fabricating smart microneedle patches. These patches can deliver insulin or other therapeutics precisely and minimally invasively. When combined with sensors, they can autonomously release drugs in response to detected glucose levels—mimicking pancreatic functions. This approach reduces patient discomfort and enhances adherence. Yet, issues like long-term stability, potential immune responses, and manufacturing scalability need further research.

5.3. Smart diagnostic biosensors

MXenes' unique electrochemical properties facilitate the development of highly sensitive biosensors capable of detecting glucose and other biomarkers with remarkable accuracy. These sensors can be integrated into wearable devices, such as patches or smart watches, providing continuous, real-time data. Their high surface area allows for the immobilization of various recognition molecules, enhancing selectivity. Nevertheless, challenges include ensuring sensor stability over time, preventing fouling, and maintaining consistent performance in biological environments.

5.4. Multifunctional platforms: combining diagnostics and therapeutics

Multifunctional platforms that integrate diagnosis and therapy are promising. For instance, MXene-based nanostructures could detect hyperglycemia and simultaneously release insulin, offering closed-loop control. These systems could incorporate nanocarriers, sensors, and actuators, creating an intelligent, autonomous management system. However, complexity in design, potential toxicity, and regulatory hurdles must be carefully navigated.

5.5. Integration with internet of things (IoT) and telemedicine

The integration of MXenes with Internet of Things (IoT) and telemedicine platforms marks a promising frontier in both diagnostic and therapeutic applications for diabetes management. These ultrathin, conductive materials are not just promising for sensors but also serve as key enablers for remote health monitoring and personalized treatment strategies. The fusion of MXene-based devices with IoT technology facilitates continuous, real-time data transmission to healthcare providers, which enhances early detection, intervention, and overall disease management. In diagnostics, MXene sensors can detect glucose and other biomarkers with exceptional sensitivity and rapid response times. When embedded into wearable patches or implantable sensors, they enable seamless monitoring without discomfort or inconvenience. These sensors, connected *via* IoT, transmit data to cloud platforms where AI algorithms analyze trends and identify potential issues. Such continuous surveillance allows for early intervention, minimizing complications and improving patient outcomes. On the therapeutic front, MXenes are also being explored for drug delivery and tissue regeneration, where their high electrochemical activity can be harnessed for smart drug release systems or stimulating tissue repair in diabetic ulcers. When paired with IoT, these therapeutic devices can be remotely controlled, adjusted, or activated based on real-time feedback, leading to more personalized and adaptive treatment regimens. Meanwhile, telemedicine platforms leverage this interconnected ecosystem, allowing healthcare providers to oversee patients remotely, make data-driven decisions, and communicate effectively. Patients benefit from increased engagement, convenience, and reduced hospital visits. Moreover, the data collected from MXene-based devices contribute to comprehensive health records, enabling more precise, tailored therapies. However, challenges persist, especially regarding data security, privacy, and regulatory compliance. Ensuring secure transmission and storage of sensitive health data remains paramount. Additionally, integrating these advanced materials within existing healthcare infrastructures requires overcoming technical, regulatory, and cost barriers.

5.6. Pancreatic beta-cell restoration

Pancreatic beta-cell restoration marks a groundbreaking development in diabetes management, with the goal of reestablishing the body's natural insulin production and potentially reversing or curing the disease. Currently, research concentrates on two primary strategies: transplanting beta cells derived from stem cells and stimulating the body's own beta-cell regeneration through processes like replication, neogenesis, or transdifferentiation. Stem cell therapies—using human embryonic stem cells (hESCs), induced pluripotent stem cells (iPSCs), and mesenchymal stem cells (MSCs)—hold significant promises for replenishing lost beta cells in diabetic patients. Concurrently, advancements in gene editing technologies, particularly CRISPR-Cas9, offer precise methods to correct genetic mutations and improve beta-cell function, paving the way for personalized regenerative treatments.[160]

6 Conclusion

MXenes have rapidly gained attention for their transformative potential in diabetes management, particularly in diagnostic and therapeutic applications. Recent advances have demonstrated MXenes' exceptional capabilities in developing highly sensitive, non-enzymatic glucose sensors and wearable biosensors that enable real-time, non-invasive monitoring of diabetes biomarkers with improved accuracy and response times. Therapeutically, MXene-based materials have shown promise in promoting wound healing, especially in diabetic foot ulcers, by modulating inflammation, scavenging reactive oxygen species, and stimulating tissue regeneration through angiogenesis and immune regulation. These multifunctional properties position MXenes as a versatile platform for next-generation diabetes care, integrating diagnostics with targeted therapy.

Despite these promising developments, several challenges remain before MXenes and their composites can be widely adopted in clinical practice. The synthesis of MXenes currently relies on hazardous chemicals and complex multi-step processes that limit scalability and raise concerns about environmental safety and production costs. Moreover, MXenes are prone to oxidation and degradation in physiological environments, which compromises their stability and long-term functionality in biomedical devices. Biocompatibility and potential toxicity issues also require thorough investigation through comprehensive *in vivo* studies to ensure safe clinical translation. Standardization of MXene production and device fabrication is essential to achieve reproducible performance and regulatory approval for medical applications. Clinical

translation of MXene-based technologies in diabetes requires rigorous validation of their safety, biocompatibility, and long-term stability through comprehensive preclinical and clinical studies to ensure effective and reliable patient outcomes.

Future perspectives for MXenes and their composites in diabetes focus on overcoming these challenges through innovative synthesis methods, surface engineering, and integration with advanced technologies. Developing scalable, environmentally friendly production techniques will be critical to meet clinical and commercial demands. Enhanced surface modifications aimed at improving oxidation resistance and biocompatibility will extend MXenes' functional lifespan in biological environments. Furthermore, combining MXenes with emerging fields such as 3D bioprinting, bioelectronics, and smart wearable systems promises to create multifunctional platforms for personalized diabetes management. Notably, the future of diabetes management is increasingly driven by the integration of AI, ML, and IoT, creating more personalized and smarter care solutions. AI-enabled continuous glucose monitoring (CGM) systems now predict blood sugar trends hours ahead, enabling timely interventions and better glycemic control. ML algorithms process large amounts of data from wearables and lifestyle inputs to customize treatment plans, optimize insulin delivery, and minimize complications—making management more proactive and precise. Additionally, IoT connectivity allows for real-time data sharing between patients and healthcare providers, enhancing remote monitoring and supporting advanced systems like artificial pancreas devices that automatically adjust insulin doses. As these technologies develop, they promise to improve patient adherence, lower healthcare costs, and foster a highly adaptive, patient-centered approach to diabetes care.

Author contributions

Meisam Samadzadeh: writing – review & editing; Mahshid Danesh: writing – review & editing; Atefeh Zarepour: writing – review & editing; Arezoo Khosravi: visualization, writing – review & editing; Siavash Iravani: supervision, conceptualization, writing – review & editing; Ali Zarrabi: supervision, writing – review & editing.

Conflicts of interest

Author(s) declare no conflict of interest.

Data availability

No primary research results, software or code have been included, and no new data were generated or analyzed as part of this review.

References

1 E. D. Abel, A. L. Gloyn, C. Evans-Molina, J. J. Joseph, S. Misra, U. B. Pajvani, J. Simcox, K. Susztak and D. J. Drucker, *Cell*, 2024, **187**, 3789–3820.
2 D. S. Rajput, S. M. Basha, Q. Xin, T. R. Gadekallu, R. Kaluri, K. Lakshmanna and P. K. R. Maddikunta, *J. Ambient Intell. Hum. Comput.*, 2022, **13**, 2829–2840.
3 A. Silva, L. Silva, I. Lopes, A. Francisco, A. Neto, M. Monteiro and H. Muela, in *Metabolic Syndrome-Lifestyle and Biological Risk Factors*, IntechOpen, 2024.
4 P. S. Hamblin, A. W. Russell, S. Talic and S. Zoungas, *Trends Endocrinol. Metabol.*, 2025, **36**, 943–954.
5 K. Rosettenstein, A. Viecelli, K. Yong, H. Do Nguyen, A. Chakera, D. Chan, G. Dogra, E. M. Lim, G. Wong and W. H. Lim, *Transplantation*, 2016, **100**, 1571–1579.
6 A. A. Al Hayek, A. A. Robert and M. A. Al Dawish, *Clin. Med. Insights: Endocrinol. Diabetes*, 2019, **12**, 1179551419861102.
7 Y. Liu, S. Zeng, W. Ji, H. Yao, L. Lin, H. Cui, H. A. Santos and G. Pan, *Adv. Sci.*, 2022, **9**, 2102466.
8 A. Shoaib, A. Darraj, M. E. Khan, L. Azmi, A. Alalwan, O. Alamri, M. Tabish and A. U. Khan, *Nanomaterials*, 2023, **13**, 867.
9 L. Chi, C. Zhang, X. Wu, X. Qian, H. Sun, M. He and C. Guo, *Biomimetics*, 2023, **8**, 167.
10 S. Maity, S. Sadhukhan, S. Ghosh and M. Das, *Discov. Chem.*, 2025, **2**, 257.
11 S. M. Mousavi, S. A. Hashemi, A. Gholami, S. Mazraedoost, W.-H. Chiang, O. Arjmand, N. Omidifar and A. Babapoor, *J. Sens.*, 2021, **2021**, 5580203.
12 F. Torabian, A. Akhavan Rezayat, M. Ghasemi Nour, A. Ghorbanzadeh, S. Najafi, A. Sahebkar, Z. Sabouri and M. Darroudi, *Biol. Trace Elem. Res.*, 2022, **200**, 1699–1709.
13 M. Asam Raza, U. Farwa, M. Waseem Mumtaz, J. Kainat, A. Sabir and A. G. Al-Sehemi, *Green Chem. Lett. Rev.*, 2023, **16**, 2275666.
14 J. Wen, N. Li, D. Li, M. Zhang, Y. Lin, Z. Liu, X. Lin and L. Shui, *ACS Appl. Nano Mater.*, 2021, **4**, 8437–8446.
15 S. Patra, K. M. Sahu, J. Mahanty and S. K. Swain, *ACS Appl. Bio Mater.*, 2023, **6**, 5730–5745.
16 Y. Wang, H. Li, A. Rasool, H. Wang, R. Manzoor and G. Zhang, *J. Nanobiotechnol.*, 2024, **22**, 1.
17 X. Lei and N. Lin, *Crit. Rev. Solid State Mater. Sci.*, 2022, **47**, 736–771.
18 Q. Wang, Y. Xian and Z. Shen, *Mater. Res. Bull.*, 2025, **196**, 113893.
19 K. C. Bhowmik, M. A. Rahman, Y. Ahmed and T. B. Hai, *Chem.–Asian J.*, 2025, **20**, e202401822.
20 A. Ali, S. M. Majhi, L. A. Siddig, A. H. Deshmukh, H. Wen, N. N. Qamhieh, Y. E. Greish and S. T. Mahmoud, *Biosensors*, 2024, **14**, 497.
21 F. Shahzad, S. A. Zaidi and R. A. Naqvi, *Crit. Rev. Anal. Chem.*, 2022, **52**, 848–864.
22 R. A. Radi, MXene Based Biosensor for the Detection of Insulin, Master's thesis, Alfaisal University, Saudi Arabia, 2024.
23 A. Zamhuri, G. P. Lim, N. L. Ma, K. S. Tee and C. F. Soon, *Biomed. Eng. Online*, 2021, **20**, 33.
24 S. S. Siwal, H. Kaur, G. Chauhan and V. K. Thakur, *Adv. NanoBiomed Res.*, 2023, **3**, 2200123.

25 V. Kumar, S. K. Shukla, M. Choudhary, J. Gupta, P. Chaudhary, S. Srivastava, M. Kumar, M. Kumar, D. K. Sarma and B. C. Yadav, *Sensors*, 2022, **22**, 5589.
26 D. Khorsandi, J.-W. Yang, Z. Ülker, K. Bayraktaroğlu, A. Zarepour, S. Iravani and A. Khosravi, *Microchem. J.*, 2024, **197**, 109874.
27 A. Hermawan, T. Amrillah, A. Riapanitra, W.-J. Ong and S. Yin, *Adv. Healthcare Mater.*, 2021, **10**, 2100970.
28 Z. Mengru, W. Qinyi, Y. Zimo, G. Bingqing, X. Zhongyu and J. Xu, *J. Mater. Sci. Mater. Med.*, 2025, **36**, 42.
29 P. Wang, Y. Wang, Y. Yi, Y. Gong, H. Ji, Y. Gan, F. Xie, J. Fan and X. Wang, *J. Nanobiotechnol.*, 2022, **20**, 259.
30 Z. Mengru, W. Qinyi, Y. Zimo, G. Bingqing, X. Zhongyu and J. Xu, *J. Mater. Sci.: Mater. Med.*, 2025, **36**, 42.
31 A. Zarepour, N. Rafati, A. Khosravi, N. Rabiee, S. Iravani and A. Zarrabi, *Nanoscale Adv.*, 2024, **6**, 3513–3532.
32 Z. Jiewen, *Int. Dent. J.*, 2025, **75**, 105287.
33 Y. Gan, B. Liang, Y. Gong, L. Wu, P. Li, C. Gong, P. Wang, Z. Yu, L. Sheng and D.-P. Yang, *Chem. Eng. J.*, 2024, **481**, 148592.
34 A. Zarepour, N. Rafati, A. Khosravi, N. Rabiee, S. Iravani and A. Zarrabi, *Nanoscale Adv.*, 2024, **6**, 3513–3532.
35 S. Pleus, A. Tytko, R. Landgraf, L. Heinemann, C. Werner, D. Müller-Wieland, A.-G. Ziegler, U. A. Müller, G. Freckmann and H. Kleinwechter, *Exp. Clin. Endocrinol. Diabetes*, 2024, **132**, 112–124.
36 I. Ahmad, S. A. Jasim, M. Sharma, R. J. S, A. Hjazi, J. S. Mohammed, A. Sinha, A. H. Zwamel, H. F. Hamzah and B. A. Mohammed, *J. Gene Med.*, 2024, **26**, e3730.
37 A. Kulkarni, A. R. Thool and S. Daigavane, *Cureus*, 2024, **16**, e56674.
38 J. Carmichael, H. Fadavi, F. Ishibashi, A. C. Shore and M. Tavakoli, *Front. Endocrinol.*, 2021, **12**, 671257.
39 R. Deepa and A. Sivasamy, *AIP Adv.*, 2023, **13**, 115307.
40 E. Zerihun, F. Abera, G. Kune, F. Girma, M. Tesgera and M. Robi, *Clin. Epidemiol. Global Health*, 2024, **25**, 101483.
41 M. J. Hossain, M. Al-Mamun and M. R. Islam, *Health Sci. Rep.*, 2024, **7**, e2004.
42 R. Setyawati, A. Astuti, T. P. Utami, S. Adiwijaya and D. M. Hasyim, *J. World Futur. Med. Health Nurs.*, 2024, **2**, 51–63.
43 A. G. Mersha, D. N. Tollosa, T. Bagade and P. Eftekhari, *J. Psychosom. Res.*, 2022, **162**, 110991.
44 A. Naseer, M. M. Khan, F. Arif, W. Iqbal, A. Ahmad and I. Ahmad, *Expert Syst.*, 2025, **42**, e13520.
45 A. Morais, A. Duarte, M. Fernandes, A. Borba, C. Ruano, I. Marques, J. Calha, J. Branco, J. Pereira and M. Salvador, *Pulmonology*, 2025, **31**, 2416840.
46 Z. U. D. Babar, V. Iannotti, G. Rosati, A. Zaheer, R. Velotta, B. Della Ventura, R. Álvarez-Diduk and A. Merkoçi, *Chem. Soc. Rev.*, 2025, **54**, 3387–3440.
47 H. Cui, L. Yang, X. Fu, G. Li, S. Xing and X.-F. Wang, *Surf. Interfaces*, 2023, **41**, 103196.
48 W. Yan, Application of immunomodulatory biomaterials for cardiovascular repair, PhD thesis, University of Manitoba, Canada, 2024.
49 R. S. Chouhan, M. Shah, D. Prakashan, R. PR, P. Kolhe and S. Gandhi, *Diagnostics*, 2023, **13**, 697.
50 S. Tian, M. Wang, P. Fornasiero, X. Yang, S. Ramakrishna, S.-H. Ho and F. Li, *Chin. Chem. Lett.*, 2023, **34**, 108241.
51 S. Shahzad, F. J. Iftikhar, A. Shah, H. A. Rehman and E. Iwuoha, *RSC Adv.*, 2024, **14**, 36713–36732.
52 Y. Du, X. Zhang, P. Liu, D.-G. Yu and R. Ge, *Front. Chem.*, 2022, **10**, 944428.
53 L.-J. Shang, S.-Q. Yu, X.-W. Shang, X.-Y. Wei, H.-Y. Wang, W.-S. Jiang and Q.-Q. Ren, *J. Appl. Electrochem.*, 2024, **54**, 1807–1817.
54 K. Saraswathi, M. S. B. Reddy, N. Jayarambabu, K. V. Rao, S. Aich and T. V. Rao, *Microchem. J.*, 2024, **205**, 111302.
55 Y. Pan, M. He, J. Wu, H. Qi and Y. Cheng, *Sens. Actuators, B*, 2024, **401**, 135055.
56 Y. Chen, H. Xiao, Q. Fan, W. Tu, S. Zhang, X. Li and T. Hu, *ACS Appl. Mater. Interfaces*, 2024, **16**, 55155–55165.
57 Y. Lei, W. Zhao, Y. Zhang, Q. Jiang, J. H. He, A. J. Baeumner, O. S. Wolfbeis, Z. L. Wang, K. N. Salama and H. N. Alshareef, *Small*, 2019, **15**, 1901190.
58 X. Cui, J. Li, Y. Li, M. Liu, J. Qiao, D. Wang, H. Cao, W. He, Y. Feng and Z. Yang, *Spectrochim. Acta, Part A*, 2022, **266**, 120432.
59 A. Perera, K. A. U. Madhushani, B. T. Punchihewa, A. Kumar and R. K. Gupta, *Materials*, 2023, **16**, 1138.
60 J. He, J. D. Butson, R. Gu, A. C. M. Loy, Q. Fan, L. Qu, G. K. Li and Q. Gu, *Adv. Sci.*, 2025, **12**, e2414674.
61 O. Ama, M. Sadiq, M. Johnson, Q. Zhang and D. Wang, *Chemosensors*, 2020, **8**, 102.
62 Y. Jin, Y. Chen, X. Li, S. Han, L. Mou and N. Li, *Bioelectrochemistry*, 2025, **163**, 108907.
63 Q. Wu, Z. Li, Q. Liang, R. Ye, S. Guo, X. Zeng, J. Hu and A. Li, *Electrochim. Acta*, 2022, **428**, 140945.
64 N. Alanazi, T. Selvi Gopal, M. Muthuramamoorthy, A. A. E. Alobaidi, R. A. Alsaigh, M. H. Aldosary, S. Pandiaraj, M. Almutairi, A. N. Grace and A. Alodhayb, *ACS Appl. Nano Mater.*, 2023, **6**, 12271–12281.
65 H. L. Chia, C. C. Mayorga-Martinez, N. Antonatos, Z. k. Sofer, J. J. Gonzalez-Julian, R. D. Webster and M. Pumera, *Anal. Chem.*, 2020, **92**, 2452–2459.
66 W. Zhang, S. Jiang, H. Yu, S. Feng and K. Zhang, *iScience*, 2025, **28**, 111737.
67 K. Saraswathi, M. S. B. Reddy, N. Jayarambabu, C. Harish, K. V. Rao and T. V. Rao, *Surf. Interfaces*, 2025, **56**, 105728.
68 T. Selvi Gopal, J. T. James, B. Gunaseelan, K. Ramesh, V. Raghavan, C. J. Malathi A, K. Amarnath, V. G. Kumar, S. J. Rajasekaran and S. Pandiaraj, *ACS Omega*, 2024, **9**, 8448–8456.
69 H. Gu, Y. Xing, P. Xiong, H. Tang, C. Li, S. Chen, R. Zeng, K. Han and G. Shi, *ACS Appl. Nano Mater.*, 2019, **2**, 6537–6545.
70 Y. Hao, M. Fang, C. Xu, Z. Ying, H. Wang, R. Zhang, H.-M. Cheng and Y. Zeng, *J. Mater. Sci. Technol.*, 2021, **66**, 57–63.
71 M. Wu, Q. Zhang, Y. Fang, C. Deng, F. Zhou, Y. Zhang, X. Wang, Y. Tang and Y. Wang, *J. Colloid Interface Sci.*, 2021, **586**, 20–29.

72 L. Feng, J. Chen, M. Yang, J. Wang, S. Yin, D. Zhang, W. Qin and J. Song, *Microchim. Acta*, 2024, **191**, 451.
73 T. S. Gopal, S. K. Jeong, T. A. Alrebdi, S. Pandiaraj, A. Alodhayb, M. Muthuramamoorthy and A. N. Grace, *Mater. Today Chem.*, 2022, **24**, 100891.
74 H. Yin, Z. Cui, L. Wang and Q. Nie, *Sens. Actuators, B*, 2016, **222**, 1018–1023.
75 R. A. Varkani, H.-A. Rafiee-Pour and M. Noormohammadi, *Microchem. J.*, 2021, **170**, 106712.
76 C. Cao, Q. Chang, H. Qiao, R. Shao, X. Guo, G. Xiao, W. Shi and L. Huang, *Sens. Actuators, B*, 2021, **340**, 129943.
77 R. Gao, X. Yang, Q. Yang, Y. Wu, F. Wang, Q. Xia and S.-J. Bao, *Microchim. Acta*, 2021, **188**, 1–9.
78 M.-H. Lin, S. Gupta, C. Chang, C.-Y. Lee and N.-H. Tai, *Microchem. J.*, 2022, **180**, 107547.
79 X. Tong, L. Jiang, Q. Ao, X. Lv, Y. Song and J. Tang, *Biosens. Bioelectron.*, 2024, **248**, 115942.
80 M. A. Zahed, M. Sharifuzzaman, H. Yoon, M. Asaduzzaman, D. K. Kim, S. Jeong, G. B. Pradhan, Y. D. Shin, S. H. Yoon and S. Sharma, *Adv. Funct. Mater.*, 2022, **32**, 2208344.
81 M. Li, L. Fang, H. Zhou, F. Wu, Y. Lu, H. Luo, Y. Zhang and B. Hu, *Appl. Surf. Sci.*, 2019, **495**, 143554.
82 Y. Xie, Y. Song, Y. Zhang, L. Xu, L. Miao, C. Peng and L. Wang, *J. Alloys Compd.*, 2018, **757**, 105–111.
83 H. Chen, Z. Mei, K. Qi, Y. Wang and R. Chen, *J. Electroanal. Chem.*, 2022, **920**, 116585.
84 L. Jothi, N. Jayakumar, S. Jaganathan and G. Nageswaran, *Mater. Res. Bull.*, 2018, **98**, 300–307.
85 Y. P. Palve and N. Jha, *Mater. Chem. Phys.*, 2020, **240**, 122086.
86 Y. Li, M. Xie, X. Zhang, Q. Liu, D. Lin, C. Xu, F. Xie and X. Sun, *Sens. Actuators, B*, 2019, **278**, 126–132.
87 V. Myndrul, E. Coy, N. Babayevska, V. Zahorodna, V. Balitskyi, I. Baginskiy, O. Gogotsi, M. Bechelany, M. T. Giardi and I. Iatsunskyi, *Biosens. Bioelectron.*, 2022, **207**, 114141.
88 L. Feng, W. Qin, Y. Wang, C. Gu, X. Li, J. Chen, J. Chen, H. Qiao, M. Yang and Z. Tian, *Microchem. J.*, 2023, **184**, 108142.
89 Q.-F. Li, X. Chen, H. Wang, M. Liu and H.-L. Peng, *ACS Appl. Mater. Interfaces*, 2023, **15**, 13290–13298.
90 M. Li, L. Wang, R. Liu, J. Li, Q. Zhang, G. Shi, Y. Li, C. Hou and H. Wang, *Biosens. Bioelectron.*, 2021, **174**, 112828.
91 J. E. Song and E. C. Cho, *Sci. Rep.*, 2016, **6**, 34622.
92 M. Farahmandpour, D. Dideban, M. M. Dehbali and Z. Kordrostami, *J. Alloys Compd.*, 2025, **1014**, 178715.
93 A. Alshraim, S. Rahman, M. Al-Gawati, A. N. Grace and A. N. Alodhayb, *Int. J. Electrochem. Sci.*, 2025, **20**, 100980.
94 S. Siraj, G. Bansal, B. Hasita, S. Srungaram, S. K. S, F. J. Rybicki, S. Sonkusale and P. Sahatiya, *ACS Appl. Nano Mater.*, 2024, **7**, 11350–11361.
95 F. Mohajer, G. M. Ziarani, A. Badiei, S. Iravani and R. S. Varma, *Micromachines*, 2022, **13**, 1773.
96 V. Shukla, *Nanoscale Adv.*, 2019, **1**, 1640–1671.
97 G. Faghani and A. Azarniya, *Heliyon*, 2024, **10**, e39611.
98 S. K. Singh, M. Paul, A. Singh, A. Sharma, M. Kumar, J. Gupta, S. Sivakumar and V. Verma, *ACS Appl. Mater. Interfaces*, 2024, **16**, 67514–67522.
99 P. Wang, Y. Wang, Y. Yi, Y. Gong, H. Ji, Y. Gan, F. Xie, J. Fan and X. Wang, *J. Nanobiotechnol.*, 2022, **20**, 259.
100 Y. Gan, B. Liang, Y. Gong, L. Wu, P. Li, C. Gong, P. Wang, Z. Yu, L. Sheng, D.-P. Yang and X. Wang, *Chem. Eng. J.*, 2024, **481**, 148592.
101 W. You, Z. Cai, F. Xiao, J. Zhao, G. Wang, W. Wang, Z. Chen, W. Hu, Y. Chen and Z. Wang, *Adv. Sci.*, 2025, **12**, 2417314.
102 Y. Zhu, H. Liu, P. Wu, Y. Chen, Z. Deng, L. Cai and M. Wu, *Theranostics*, 2024, **14**, 7140–7198.
103 J. Gong, S. Lai, S. Zhang, K. Liang and Y. Deng, *Small*, 2025, **21**, 2409437.
104 J. Fu, D. Wang, Z. Tang, Y. Xu, J. Xie, R. Chen, P. Wang, Q. Zhong, Y. Ning and M. Lei, *J. Nanobiotechnol.*, 2024, **22**, 384.
105 Y.-J. Hsu, A. Nain, Y.-F. Lin, Y.-T. Tseng, Y.-J. Li, A. Sangili, P. Srivastava, H.-L. Yu, Y.-F. Huang and C.-C. Huang, *J. Nanobiotechnol.*, 2022, **20**, 235.
106 H. Zhou, L. Chen, C. Huang, Z. Jiang, H. Zhang, X. Liu, F. Zhu, Q. Wen, P. Shi, K. Liu and L. Yang, *J. Nanobiotechnol.*, 2024, **22**, 530.
107 G. Guo, Z. Liu, J. Yu, Y. You, M. Li, B. Wang, J. Tang, P. Han, J. Wu and H. Shen, *Adv. Mater.*, 2024, **36**, 2310320.
108 X. Jiang, J. Ma, K. Xue, J. Chen, Y. Zhang, G. Zhang, K. Wang, Z. Yao, Q. Hu, C. Lin, B. Lei and C. Mao, *ACS Nano*, 2024, **18**, 4269–4286.
109 S. K. Singh, M. Paul, A. Singh, A. Sharma, M. Kumar, J. Gupta, S. Sivakumar and V. Verma, *ACS Appl. Mater. Interfaces*, 2024, **16**, 67514–67522.
110 J. Wang, Y. Wang, M. Lu, X. Cao, M. Xia, M. Zhao and Y. Zhao, *Aggregate*, 2025, **6**, e700.
111 D. Liu, S. Bi, H. Wang, J. Gu and S. Wang, *Composites, Part A*, 2024, **180**, 108065.
112 Y. Gong, W. Qi, W. Lu, Q. Chang, Y. Xie, J. Wang and X. Deng, *J. Colloid Interface Sci.*, 2025, **689**, 137247.
113 X. Qiu, L. Nie, P. Liu, X. Xiong, F. Chen, X. Liu, P. Bu, B. Zhou, M. Tan, F. Zhan, X. Xiao, Q. Feng and K. Cai, *Biomaterials*, 2024, **308**, 122548.
114 Z. Liu, X. Chen, B. Jin, W. Wei, Y. Zhang, X. Wang, Z. Xiang, T. Zhang and P.-L. Tremblay, *Chem. Eng. J.*, 2025, **503**, 158615.
115 X. Ou, Z. Yu, X. Zheng, L. Chen, C. Pan, D. Li, Z. Qiao and X. Zheng, *Mater. Today Bio*, 2025, **31**, 101538.
116 Y. Li, R. Fu, Z. Duan, C. Zhu and D. Fan, *ACS Nano*, 2022, **16**, 7486–7502.
117 X. Yang, C. Zhang, D. Deng, Y. Gu, H. Wang and Q. Zhong, *Small*, 2022, **18**, e2104368.
118 J. Wang, J. He, R. Zhou, R. Zeng, S. Guan, X. Yang, Z. Liu, Y. Liu, X. Zhu, Q. Liao, Y. Yang, H. Dai and J. Zhou, *ACS Appl. Nano Mater.*, 2025, **8**, 5466–5480.
119 T. Amrillah, C. A. Che Abdullah, A. Hermawan, F. N. Indah Sari and V. N. Alviani, *Nanomaterials*, 2022, **12**, 4280.
120 S. Iravani, *Ceram. Int.*, 2022, **48**, 24144–24156.
121 J. Cui, J. Wu, A. Feng, Y. Yu, L. Mi and Y. Yu, *Chem. Eng. J.*, 2024, **493**, 152289.

122 J. E. Heckler, G. R. Neher, F. Mehmood, D. B. Lioi, R. Pachter, R. Vaia, W. J. Kennedy and D. Nepal, *Langmuir*, 2021, **37**, 5447–5456.
123 P. Wan, Y. Chen and Q. Tang, *ChemPhysChem*, 2024, **25**, e202400325.
124 F. Cao, Y. Zhang, H. Wang, K. Khan, A. K. Tareen, W. Qian, H. Zhang and H. Ågren, *Adv. Mater.*, 2022, **34**, 2107554.
125 P. Eghbali, A. Hassani, S. Wacławek, K.-Y. A. Lin, Z. Sayyar and F. Ghanbari, *Chem. Eng. J.*, 2023, **480**, 147920.
126 R. A. Soomro, P. Zhang, B. Fan, Y. Wei and B. Xu, *Nano–Micro Lett.*, 2023, **15**, 108.
127 C. J. Zhang, S. Pinilla, N. McEvoy, C. P. Cullen, B. Anasori, E. Long, S.-H. Park, A. Seral-Ascaso, A. Shmeliov, D. Krishnan, C. Morant, X. Liu, G. S. Duesberg, Y. Gogotsi and V. Nicolosi, *Chem. Mater.*, 2017, **29**, 4848–4856.
128 Z. Zheng, C. Guo, E. Wang, Z. He, T. Liang, T. Yang and X. Hou, *Inorg. Chem. Front.*, 2021, **8**, 2164–2182.
129 L. Yao, L. Qian, W. Song, S. Zhang, Y. Zhang, L. Zhang, X. Li, G. Yan and V. Nica, *ACS Appl. Mater. Interfaces*, 2024, **16**, 48147–48162.
130 J. Yang, Q. Dai, H. Wu, L. Yang, S. Guo, Q. Zhao, M. Hou, S. Komarneni and Y. Xia, *Molecules*, 2025, **30**, 4440.
131 T. Akram, B. Zhang and G. Zhao, *Adv. Mater. Technol.*, 2025, e00906.
132 L. Liu, M. Gao, X. Fan, Z. Lu and Y. Li, *J. Colloid Interface Sci.*, 2025, **684**, 469–480.
133 S. Sun, R. Yuan, S. Ling, T. Zhou, Z. Wu, M. Fu, H. He, X. Li and C. Zhang, *ACS Appl. Mater. Interfaces*, 2024, **16**, 7826–7837.
134 B. Farasati Far, N. Rabiee and S. Iravani, *RSC Adv.*, 2023, **13**, 34562–34575.
135 G. P. Lim, C. F. Soon, N. L. Ma, M. Morsin, N. Nayan, M. K. Ahmad and K. S. Tee, *Environ. Res.*, 2021, **201**, 111592.
136 M. Asadi Tokmedash and J. Min, *ACS Appl. Mater. Interfaces*, 2024, **16**, 21415–21426.
137 J. Huang, J. Su, Z. Hou, J. Li, Z. Li, Z. Zhu, S. Liu, Z. Yang, X. Yin and G. Yu, *Chem. Res. Toxicol.*, 2023, **36**, 347–359.
138 J. Nowak-Jary and B. Machnicka, *Int. J. Nanomed.*, 2023, **18**, 4067–4100.
139 J. Wu, Y. Yu and G. Su, *Nanomaterials*, 2022, **12**, 828.
140 T. R. Dmytriv and V. I. Lushchak, *Chem. Rec.*, 2024, **24**, e202300338.
141 A. Iqbal, J. Hong, T. Y. Ko and C. M. Koo, *Nano Convergence*, 2021, **8**, 9.
142 H. Huang, L. Cui, P. Zhang, Y. Zhang, C. Wang, C. Sun, Z. Zhou, X. Liu, W. Zhou, B. Ma, H. Liu and S. Wang, *Sci. China Mater.*, 2025, 1–6.
143 T. R. Dmytriv and V. I. Lushchak, *Chem. Rec.*, 2024, **24**, e202300338.
144 A. M. Jastrzębska, A. Szuplewska, T. Wojciechowski, M. Chudy, W. Ziemkowska, L. Chlubny, A. Rozmysłowska and A. Olszyna, *J. Hazard. Mater.*, 2017, **339**, 1–8.
145 S. Sagadevan and W.-C. Oh, *J. Drug Delivery Sci. Technol.*, 2023, **85**, 104569.
146 I. A. Vasyukova, O. V. Zakharova, D. V. Kuznetsov and A. A. Gusev, *Nanomaterials*, 2022, **12**, 1797.
147 J. Sengupta and C. M. Hussain, *Biosensors*, 2025, **15**, 127.
148 K. N. Alagarsamy, L. R. Saleth, K. Diedkova, V. Zahorodna, O. Gogotsi, M. Pogorielov and S. Dhingra, *Nanoscale*, 2025, **17**, 11785–11811.
149 S. R. Averbeck, D. Xu, B. B. Murphy, K. Shevchuk, S. Shankar, M. Anayee, M. Der Torossian Torres, M. S. Beauchamp, C. de la Fuente-Nunez, Y. Gogotsi and F. Vitale, *ACS Nano*, 2023, **17**, 9442–9454.
150 M. Pogorielov, A. Yilmazer, L. G. Delogu and Y. Gogotsi, *Nanoscale*, 2025, **17**, 11781–11784.
151 Z. U. D. Babar, B. D. Ventura, R. Velotta and V. Iannotti, *RSC Adv.*, 2022, **12**, 19590–19610.
152 A. Khunger, N. Kaur, Y. K. Mishra, G. R. Chaudhary and A. Kaushik, *Mater. Lett.*, 2021, **304**, 130656.
153 D. Lu, H. Zhao, X. Zhang, Y. Chen and L. Feng, *Biosensors*, 2022, **12**, 820.
154 M. Xin, J. Li, Z. Ma, L. Pan and Y. Shi, *Front. Chem.*, 2020, **8**, 297.
155 S. Iravani and R. S. Varma, *Nano–Micro Lett.*, 2022, **14**, 213.
156 F. Mohajer, G. M. Ziarani, A. Badiei, S. Iravani and R. S. Varma, *Nanomaterials*, 2023, **13**, 345.
157 B. M. Ilfeld, J. C. Eisenach and R. A. Gabriel, *Anesthesiology*, 2021, **134**, 283–344.
158 T. A. Tabish, M. Z. I. Pranjol, F. Jabeen, T. Abdullah, A. Latif, A. Khalid, M. Ali, H. Hayat, P. G. Winyard, J. L. Whatmore and S. Zhang, *Appl. Mater. Today*, 2018, **12**, 389–401.
159 M. Sharifiaghdam, E. Shaabani, R. Faridi-Majidi, S. C. De Smedt, K. Braeckmans and J. C. Fraire, *Mol. Ther.*, 2022, **30**, 2891–2908.
160 M. Mohamed and I. Abdalla, *World J. Gastroenterol.*, 2024, **30**, 4339–4353.